



1 **High number concentrations of transparent exopolymer particles (TEP) in**  
2 **ambient aerosol particles and cloud water – A case study at the tropical**  
3 **Atlantic Ocean**

4  
5 **Manuela van Pinxteren<sup>1</sup>, Tiera-Brandy Robinson<sup>2</sup>, Sebastian Zeppenfeld<sup>1</sup>, Xianda Gong<sup>3+</sup>,**  
6 **Enno Bahlmann<sup>4</sup>, Kanneh Wadinga Fomba<sup>1</sup>, Nadja Triesch<sup>1</sup>, Frank Stratmann<sup>3</sup>, Oliver Wurl<sup>2</sup>,**  
7 **Anja Engel<sup>5</sup>, Heike Wex<sup>3</sup>, Hartmut Herrmann<sup>1\*</sup>**

8  
9 \*Corresponding author: Hartmut Herrmann ([herrmann@tropos.de](mailto:herrmann@tropos.de))

10  
11 <sup>1</sup> Atmospheric Chemistry Department (ACD), Leibniz-Institute for Tropospheric Research  
12 (TROPOS), 04318 Leipzig, Germany

13 <sup>2</sup> Institute for Chemistry and Biology of the Marine Environment, Carl-von-Ossietzky  
14 University Oldenburg, 26382 Wilhelmshaven, Germany

15 <sup>3</sup> Dept. of Experimental Cloud and Microphysics, Leibniz-Institute for Tropospheric Research  
16 (TROPOS), 04318 Leipzig, Germany

17 + now at: Center for Aerosol Science and Engineering, Department of Energy, Environmental  
18 and Chemical Engineering, Washington University in St. Louis, 63130, MO, USA

19 <sup>4</sup> Leibniz Centre for Tropical Marine Research (ZMT), 28359 Bremen, Germany

20 <sup>5</sup> GEOMAR Helmholtz Centre for Ocean Research, Kiel 24105, Germany

21

22

23

24

25

26

27

28

29

30

31

32

33



34 Abstract

35 Transparent exopolymer particles (TEP) exhibit the properties of gels and are ubiquitously  
36 found in the world oceans. Possibly, TEP may enter the atmosphere as part of sea spray  
37 aerosol. Here, we report number concentrations of TEP (diameter > 4.5  $\mu\text{m}$ ) in ambient aerosol  
38 and cloud water samples from the tropical Atlantic Ocean as well as in generated aerosol  
39 particles using a plunging waterfall tank that was filled with the ambient sea water. The  
40 ambient TEP concentrations ranged between  $7 \times 10^2$  and  $3 \times 10^4$  #TEP  $\text{m}^{-3}$  in supermicron  
41 aerosol particles and correlations to sodium ( $\text{Na}^+$ ) and calcium ( $\text{Ca}^{2+}$ ) ( $R^2 = 0.5$ ) suggested some  
42 contribution via bubble bursting. Cloud water TEP concentrations were between  $4 \times 10^6$  and  
43  $9 \times 10^6$  #TEP  $\text{L}^{-1}$  corresponding to equivalent air concentrations of  $2 - 4 \times 10^3$  #TEP  $\text{m}^{-3}$ . The TEP  
44 concentrations in the tank-generated aerosol particles, produced from the same waters and  
45 sampled with an equivalent system, were significantly lower ( $4 \times 10^2 - 2 \times 10^3$  #TEP  $\text{m}^{-3}$ )  
46 compared to the ambient concentrations.

47 Based on  $\text{Na}^+$  concentrations in seawater and in the atmosphere, the enrichment factor for  
48 TEP in the atmosphere was calculated. The tank-generated TEP were enriched by a factor of  
49 50 compared to sea water and, therefore, in-line with published enrichment factors for  
50 supermicron organic matter in general and TEP specifically. TEP enrichment in the ambient  
51 atmosphere was on average  $1 \times 10^3$  in cloud water and  $9 \times 10^3$  in ambient aerosol particles and  
52 therefore about two orders of magnitude higher than the corresponding enrichment from the  
53 tank study. Such high enrichment of supermicron particulate organic constituents in the  
54 atmosphere is uncommon and we propose that atmospheric TEP concentrations resulted  
55 from a combination of enrichment during bubble bursting transfer from the ocean and TEP in-  
56 situ formation in atmospheric phases. Abiotic in-situ formation might have occurred from  
57 aqueous reactions of dissolved organic precursors that were present in particle and cloud  
58 water samples, while biotic formation involves bacteria, which were abundant in the cloud  
59 water samples.

60 The ambient TEP number concentrations were two orders of magnitude higher than recently  
61 reported ice nucleating particle (INP) concentrations measured at the same location. As TEP  
62 likely possess good properties to act as INP, in future experiments it is worth studying if a  
63 certain part of TEP contributes a fraction of the biogenic INP population.

64

65 Keywords: Transparent exopolymer particles, marine aerosol particles, cloud water, plunging  
66 waterfall tank, ice nucleating particles, Atlantic Ocean, Cape Verde Atmospheric Observatory  
67 (CVAO)

68

69

70



## 71 1 Introduction

72 In marine ecosystems, polymer gels and gel-like material play an important role in the  
73 biochemical cycling of organic matter (OM) (Passow, 2000, 2002b). One type of gel-like  
74 particles, transparent exopolymer particles (TEP), have increasingly received attention. TEP  
75 exist as individual particles rather than diffuse exopolymeric organic material and are  
76 operationally defined as particles that are stained on 0.2 or 0.4  $\mu\text{m}$  pore-sized polycarbonate  
77 filters with the dye Alcian Blue (Passow, 2002b). TEP have shown surface-active properties  
78 and are highly hydrated molecules (Passow et al. 2002a). Chemically, they consist of  
79 polysaccharide chains including uronic acids or sulphated monosaccharides that are bridged  
80 with divalent cations (mostly calcium) (Alldredge et al., 1993; Bittar et al., 2018).

81 In contrast to solid particles, TEP contain properties of gels; with similar constituents  
82 (carrageenans, alginic acid, and xanthan) to those that form gels, spontaneously forming from  
83 dissolved fibrillar colloids, and they can be broken up by Calcium chelators such as EDTA.  
84 However, because TEP have not yet been seen to undergo phase transition they can officially  
85 only be classified as gel-like particles (Verdugo et al., 2004). Regardless though, TEP have been  
86 shown to be highly important in sedimentation processes and carbon cycling in the sea (Mari  
87 et al., 2017), as well as highly prevalent in the sea surface microlayer (SML) (Robinson et al.,  
88 2019a) with a potentially significant effect on air-sea release of marine aerosols.

89 Generally, TEP can be formed via two pathways. First, the biotic pathway happens via  
90 a breakdown and secretion of precursor material from an organism or via a direct release as  
91 particles from aquatic organisms, e.g. as metabolic-excess waste products when nutrients are  
92 limited (Decho and Gutierrez, 2017; Engel et al., 2004; Engel et al., 2002). High TEP  
93 concentrations are usually associated with phytoplankton blooms, with the majority of  
94 precursor material being released by diatoms and to a lesser extent other plankton species.  
95 However, bacteria are also associated with TEP production, although their exact role is still  
96 not resolved (Passow, 2002a). Secondly, TEP form through abiotic pathways. These could be  
97 spontaneous formation from dissolved organic precursors (e.g. dissolved polysaccharides)  
98 that are released by aquatic organisms. The abiotic formation is enhanced by turbulent or  
99 laminar shear (Engel et al., 2002; Passow, 2000). Recent studies confirmed that higher wind  
100 speeds, forming breaking waves, could be an effective transport and formation mechanism  
101 for TEP to the ocean surface (Robinson et al., 2019b).

102 TEP are highly sticky and provide surfaces for other molecules and bacterial colonization  
103 (Passow, 2002b), with between 0.5 and 25% (on average 3%) of marine bacteria being  
104 attached to TEP (Busch et al., 2017). TEP naturally aggregate to other particles or highly dense  
105 matter and can sink in the ocean to contribute to downward carbon fluxes. However, TEP  
106 which are not attached to sufficiently dense material will have a resulting low density and rise  
107 to the surface to form or stabilize the SML which links the oceans with the atmosphere (Wurl  
108 and Holmes, 2008).

109 From the ocean surface, TEP have the potential to be transferred to the atmosphere.  
110 Recently, high TEP mass concentrations of  $1.4 \mu\text{g m}^{-3}$  were reported in ambient marine aerosol



111 particles measured in a size range between 0.1 and 1  $\mu\text{m}$ , suggesting that gel-like particles can  
112 constitute more than half of the particulate OM mass (Aller et al., 2017).

113 Ocean-derived OM, of which TEP is a part, has been reported to be enriched and  
114 selectively transferred (compared to sea salt) to the atmosphere (Facchini et al., 2008;Keene  
115 et al., 2007;van Pinxteren et al., 2017). Compared to seawater concentrations, organic mass  
116 in submicron aerosol particles is strongly enriched by factors of  $10^3$  and  $10^4$  (partly up to  $10^5$ )  
117 (Quinn et al., 2015 and references therein) due to (not yet in detail resolved) processes during  
118 the rise and burst of bubbles at the ocean surface (Blanchard, 1975). The enrichment of OM  
119 in supermicron aerosol particles is significantly lower, with average aerosol enrichment factors  
120 of  $10^2$  (Hoffman and Duce, 1976;Keene et al., 2007;Quinn et al., 2015). Aerosol enrichments  
121 have been studied for several organic compound groups such as lipids, carbohydrates, and  
122 proteins (e.g. Gao et al., 2012;Rastelli et al., 2017;Schmitt-Kopplin et al., 2012;Triesch et al.,  
123 2021a;Triesch et al., 2021b;Zeppenfeld et al., 2021). However, at current, data for TEP  
124 enrichment in the atmosphere are scarce. Aller et al. (2017) presented TEP mass  
125 concentrations in size-resolved aerosol particles and found them to contain more TEP for  
126 submicron sizes than for larger sizes. Kuznetsova et al. (2005) reported TEP enrichment of a  
127 factor of 40 in freshly produced sea spray. Besides TEP, other types of gel-like airborne  
128 particles in the size range of 100 – 300 nm (and even smaller) have been observed, e.g. in the  
129 Arctic atmosphere likely originating from the ocean surface (Bigg and Leck, 2008;Leck and  
130 Bigg, 2005b, a).

131 In addition to an oceanic transfer, atmospheric in-situ formation might contribute to  
132 OM abundance in the atmosphere. Ervens and Amato (2020) provided a framework to  
133 estimate the production of secondary biological aerosol mass in clouds by microbial cell  
134 growth and multiplication. It was recently shown that this pathway might represent a  
135 significant source of biological aerosol material (Ervens and Amato, 2020;Khaled et al.,  
136 2021;Zhang et al., 2021). In another recent study, cloud water in-situ formation of amino acids  
137 resulting from biotic and abiotic processes has been measured and modelled (Jaber et al.,  
138 2021). Moreover, a higher microbial enzymatic activity on the aerosol particles compared to  
139 seawater was observed and it was hypothesised that after ejection from the ocean, active  
140 enzymes can dynamically influence the OM concentration and composition of marine aerosol  
141 particles (Malfatti et al., 2019). Still, the atmospheric in-situ formation of important OM  
142 compounds and its importance is not well investigated to date and no studies exist about  
143 atmospheric in-situ TEP formation.

144 Regarding the properties of ocean-derived OM in the atmosphere, its ability to act as  
145 cloud condensation nuclei (CCN) (Orellana et al., 2011;Sellegrri et al., 2021) or ice nucleating  
146 particle (INP) (Burrows et al., 2013;Gong et al., 2020a;McCluskey et al., 2018a;McCluskey et  
147 al., 2018b) is not well understood at present. Bigg and Leck, (2008) and Leck and Bigg (2005a)  
148 demonstrated, based on morphology and chemical properties, that the biogenic particles  
149 collected in air and in the surface microlayer could be consistent with polymer gels. For regions  
150 that generally show a low total particle number concentration and low CCN (such as the high



151 Arctic), it was suggested that microgels are CCN (Leck and Bigg, 2005b, a; Orellana et al., 2011),  
152 due to their hydrated and hygroscopic nature and due to the absence of other significant  
153 aerosol particle sources.

154 In addition, oceanic biogenic INP sources have been discussed (Creamean et al.,  
155 2019; Hartmann et al., 2020; Wilson et al., 2015; Zeppenfeld et al., 2019). In regions, however,  
156 where other sources dominate, oceanic sources might not suffice to explain the INP  
157 population, and non-marine sources most likely significantly contributed to the local INP  
158 concentration (Gong et al., 2020a). According to their structure, biopolymers consisting of  
159 proteins, lipids, and higher saccharides have been shown to play a role in the ice-nucleating  
160 activity (Pummer et al., 2015). In this context, TEP might provide excellent functionalities to  
161 act as INP, as they form a 3D network where water molecules can attach, providing a  
162 structured surface for ice formation. A direct link between TEP and INP, however, has not yet  
163 been experimentally shown in field studies.

164 Within the present study, the number concentrations and size distributions of TEP in  
165 the ambient atmosphere in the tropical Atlantic Ocean were elucidated. We aimed at  
166 investigating the TEP number concentrations in the ambient aerosol particles and cloud water  
167 and to derive connections to oceanic transfer and potential in-situ formation mechanisms.  
168 Finally, we compared the TEP number concentrations with recently published atmospheric  
169 INP number concentrations at the same location (Gong et al., 2020a) and analyse possible  
170 interconnections. To our knowledge, this is the first study with detailed measurements of TEP  
171 number size distribution in different atmospheric marine compartments in the tropical  
172 Atlantic environment.

173

## 174 2 Material and methods

### 175 2.1 Measurement site and ambient sampling

176 Samples were taken during the MarParCloud: “Marine biological production, organic  
177 aerosol particles and marine clouds: a Process chain” campaign that took place from  
178 September 13<sup>th</sup> to October 13<sup>th</sup> 2017 at the Cape Verde archipelago Island Sao Vicente located  
179 in the Eastern Tropical North Atlantic (ETNA). A detailed overview of the campaign,  
180 background, goals, and first results is available in van Pinxteren et al. (2020). Measurements  
181 were performed at the Cape Verde Atmospheric Observatory (CVAO) as described in more  
182 detail elsewhere (Triesch et al., 2021a; Triesch et al., 2021b; van Pinxteren et al., 2020). The  
183 CVAO is located directly at the shoreline at the northeastern tip of the São Vicente island at  
184 10 m a.s.l (Carpenter et al., 2010; Fomba et al., 2014). Due to the trade winds, this site is free  
185 from local island pollution and provides reference conditions for studies of ocean-atmosphere  
186 interactions as there is a constant north-westerly wind from the open ocean towards the  
187 observatory. However, it also lies within the Saharan dust outflow corridor, and mainly in the  
188 winter months (January and February), dust outbreaks frequently occur.



189 Total suspended aerosol particle (TSP) for TEP analysis and PM<sub>10</sub> sampling for analysis  
190 of further aerosol constituents (inorganic ions, INP, dust) was performed on top of a 30 m  
191 sampling tower of the CVAO. Tower measurements there mainly represent the conditions  
192 above the ocean because the internal boundary layer (IBL), which can form when air passes a  
193 surface with changing roughness (i.e. the transfer from open water to island), is mainly  
194 beneath 30 m (Niedermeier et al., 2014). During the MarParCloud campaign, the marine  
195 boundary layer (MBL) was well mixed as indicated by an almost uniform particle number size  
196 distribution within the MBL (Gong et al., 2020b; van Pinxteren et al., 2020). Information on the  
197 meteorological conditions during the sampling period is given in **Tab. S1**.

198 TSP were sampled with a filter sampler consisting of a filter holder equipped with a  
199 0.2 µm pore-sized, acid-cleaned polycarbonate (PC) filter mounted to a pump. Sampling  
200 usually took place for 24 h and the flow of the pump was between 5 and 10 L min<sup>-1</sup> and  
201 frequently measured with a flowmeter. Total volumes between 10 and 15 m<sup>3</sup> were sampled.  
202 In seawater TEP analysis, filtration is usually performed at a gentle pressure of 0.2 bar (Engel,  
203 2009) which corresponds to a max flow rate of 21 or 38 L min<sup>-1</sup>. The flow rate of aerosol  
204 sampling was max. 10 L min<sup>-1</sup> and therefore TEP losses during aerosol particle sampling were  
205 not expected.

206 PM<sub>10</sub> particles were sampled with a high volume sampler (Digital, Riemer, Germany)  
207 equipped with preheated (105 °C for 24 h) 150 mm quartz fiber filters (Munktell, MK 360) at  
208 a flow rate of 700 L min<sup>-1</sup>, described in detail elsewhere (van Pinxteren et al., 2020). The  
209 sampling times for TSP as well as PM<sub>10</sub> were usually set to 24 h.

210 Cloud water was sampled on Mt. Verde, which is the highest point of the São Vicente  
211 Island (744 m), situated in the northeast of the Island (16°52.11'N, 24°56.02'W) and northwest  
212 to the CVAO (van Pinxteren et al., 2020). Again, Mt. Verde experiences direct trade winds from  
213 the ocean with no significant influence of anthropogenic activities from the island (Carpenter  
214 et al., 2010). Bulk cloud water was collected using a compact Caltech Active Strand Cloudwater  
215 Collectors (CASCC2) equipped with acid cleaned Teflon® strands (508 µm diameter). Cloud  
216 droplets were caught on the strands and gravitationally channelled into an acid-precleaned  
217 Nalgene bottle. The 50% lower size cut for the CASCC2 is approximately 3.5 µm diameter.  
218 Much of the liquid water content (LWC) in clouds is contained of drops between 10 and 30 µm  
219 diameter and the CASCC2 is predicted to collect drops in this size range with an efficiency  
220 greater than 80% (Demoz et al., 1996).

221 Three cloud water samples collected on the 20.09.2017, the 28.09.2017, and the  
222 4.10.2017 were analysed for the TEP number concentrations. They were filtered (150-200 mL)  
223 through 0.2 µm pore-sized, acid-cleaned filters for TEP analysis using the same filter type and  
224 conditions as applied for the aerosol particle staining.

225

226 2.2. Particle sampling from the plunging waterfall tank



227 To investigate a direct oceanic transfer of TEP via bubble bursting, TSP particles were  
228 sampled from a plunging waterfall tank experiment that is described in detail in the  
229 MarParCloud overview paper (van Pinxteren et al., 2020, SI section). The tank was designed  
230 to study the bubble-driven transfer of organic matter from the bulk water into the aerosol  
231 phase. It consists of a 1400 L basin with a 500 L aerosol chamber on top. The bubble driven  
232 transport of organic matter was induced using a skimmer on a plunging waterfall. A stainless  
233 steel inlet was inserted in the headspace of the tank and connected with three filter holders  
234 for offline aerosol particle sampling without size segregation (TSP). The filter system for TEP  
235 analysis was equipped with a 0.2  $\mu\text{m}$  pore-sized, acid-cleaned polycarbonate (PC) filter  
236 mounted to a pump. Sampling usually took place for  $\sim 24$  h, the flow of the pump was between  
237 5 and 10  $\text{L min}^{-1}$  and frequently measured with a flowmeter. Total volumes between 9 and  
238 10  $\text{m}^3$  were sampled. The sampling procedure was therefore identical to the ambient TEP filter  
239 sampling. Another filter holder was equipped with a preheated 47 mm quartz fiber filter  
240 (Munktell, MK 360) for sodium analysis. The stainless steel inlet was additionally connected  
241 to a TROPOS-type Scanning Mobility Particle Sizer (Wiedensohler et al., 2012) for online  
242 aerosol measurements. This method of aerosol generation resulted in an efficient generation  
243 of nascent sea-spray aerosol particles with an aerosol particle size distribution centred around  
244 100 nm (van Pinxteren et al. 2020).

245

### 246 2.3 Analysis

247 The filters obtained from ambient and tank-generated TSP aerosol particle sampling  
248 and cloud water filtrations were stained with 3 mL of an Alcian blue stock solution stained  
249 (0.02 g Alcian blue in 100 mL of acetic acid solution, pH 2.5) for 5 s yielding an insoluble non-  
250 ionic pigment and afterward rinsed with milliQ water. The dye Alcian blue consists of a  
251 macromolecule with a central copper phthalocyanine ring linked to four isothiuronium  
252 groups via thioether bonds (Passow and Alldredge, 1995). The isothiuronium groups are  
253 strong bases and account for the cationic nature. The exact staining mechanism is not resolved  
254 but it is believed that the cationic isothiuronium groups bond via electrostatic linkages (ionic  
255 bonds) with the polyanionic molecules of the TEP molecule, hence the carboxylic and sulfonic  
256 side groups are stained. Alcian Blue can also react with carbohydrate-conjoined proteins at  
257 proteoglycans, but not with nucleic acids and neutral biopolymers (Villacorte et al., 2015).  
258 After staining the filters were kept at  $-20^\circ\text{C}$  and transported to the laboratories of TROPOS.

259 For microscopic analysis, the protocol following Engel (2009) was applied. In short,  
260 abundance, area, and size-frequency distribution of TEP were determined using a light  
261 microscope (Zeiss Axio Scope A.1) connected to a camera (ColorView III). Filters were screened  
262 at 200 $\times$  magnification. About 10 pictures were taken randomly from each filter in two  
263 perpendicular cross-sections (5 pictures each cross-section; dimension 2576 x 1932 pixel, 8-  
264 bit color depth) and microscopic pictures of TEP in cloud water are shown in **Fig. 1**. Images  
265 were then semi-automatically analyzed using ImageJ (Version 1.44). A minimum threshold





266 value of  $16 \mu\text{m}^2$  was set for particle size during particle analysis to remove the detection of  
267 non-aggregate material by the program. This resulted in a minimum particle size of  $4.5 \mu\text{m}$   
268 (assuming spherical particle).

269

270 **Insert Figure 1**

271

272 Blank filters were taken for aerosol sampling (inserting filters in the aerosol sampler  
273 without probing them) and cloud water (filtering reagent water over a pre-cleaned filter),  
274 stained and treated the same way as the microscopic analysis. Blank number concentrations  
275 were on average 6% of the cloud water results and between 5% and 20% for aerosol results  
276 and the blank values were subtracted from the samples.

277 The analysis of inorganic ions from  $\text{PM}_{10}$  samples was performed with ion  
278 chromatography and conductivity detection. Aqueous extracts of the aerosol samples were  
279 made by ca. 25% of the  $\text{PM}_{10}$  filter in 1.5 mL ultra-pure water (resistivity =  $18.2 \text{ M}\Omega \text{ cm}$ ) for  
280 one hour. After the filtration ( $0.45 \mu\text{m}$  syringe filter) of the extracts sodium ( $\text{Na}^+$ ), calcium  
281 ( $\text{Ca}^{2+}$ ), magnesium ( $\text{Mg}^{2+}$ ), were analyzed by using ion chromatography (Dionex ICS-6000,  
282 Thermo Scientific). The cations were separated in an isocratic mode (eluent: 36 mM  
283 methanesulfonic acid) on a Dionex IonPac CS16- $4\mu\text{m}$  column ( $2\times 250 \text{ mm}$ ) that was combined  
284 with a Dionex IonPac CG16- $4\mu\text{m}$  guard column ( $2\times 50 \text{ mm}$ ). The detection limits for the  
285 determined ions were between 5 and  $20 \mu\text{g L}^{-1}$  (Zeppenfeld et al., 2021).

286 Non-sea-salt calcium was calculated from the ion ratio of  $\text{Ca}^{2+}/\text{Na}^+$  in seawater of  
287 0.038 (Turekian, 1968). Dust concentrations were estimated from the aerosol particle mass  
288 concentrations as the residual mass after the subtraction of all analytical concentrations from  
289 the  $\text{PM}_{10}$  mass as described elsewhere (Fomba et al., 2014). Trace metal content was  
290 determined using a Total Reflection X-Ray Fluorescence (TXRF) S2 PICOFOX (Bruker AXS,  
291 Berlin, Germany) spectrometer equipped with a Molybdenum X-ray source (Fomba et al.,  
292 2013). The cloud LWC was measured with a particle volume monitor (PVM-100, Gerber  
293 Scientific, USA), which was mounted at the same height as the cloud water samplers.

294 INP number concentration ( $N_{\text{INP}}$ ) were measured with two droplet freezing techniques  
295 (LINA: Leipzig Ice Nucleation Array and INDA: Ice Nucleation Droplet Array) in different marine  
296 compartments. The uncertainties of  $N_{\text{INP}}$  are given by the 5% to 95% confidence interval and  
297 the results are presented in (Gong et al., 2020a).

298 All the samples of this study are summarized in Table 1. In addition to samples from  
299 the MarParCloud campaign, surface seawater samples obtained from the ETNA (Engel et al.  
300 2020) were considered.

301 **Insert Table 1**

302 2.4 Enrichment factor





303 To determine enrichment or depletion of TEP in the atmosphere (i.e. on the aerosol  
304 particles and in the cloud water) in relation to the TEP concentration in the ocean water, the  
305 concept of the aerosol enrichment factor can be applied. To this end, the concentration of the  
306 compound of interest in each compartment is related to the respective sodium mass  
307 concentration, as sodium is regarded as a conservative sea salt tracer transferred to the  
308 atmosphere in the process of bubble bursting (Sander et al., 2003). This concept is usually  
309 applied for calculating the enrichment of a compound in the aerosol particles ( $EF_{aer.}$ ) in relation  
310 to seawater (Quinn et al., 2015), but was recently extended to calculate the enrichment of  
311 organic compounds in cloud water ( $EF_{cloud}$ ) in relation to seawater (Triesch et al., 2021a).  
312 Therefore, in the following the enrichment factor is defined as  $EF_{atm.}$  (atmosphere  
313 enrichment factor) in equation 1.

314

$$315 \quad EF_{atm.} = \frac{c(TEP)_{atm}/c(Na^{+}mass)_{atm}}{c(TEP)_{seawater}/c(Na^{+}mass)_{seawater}} \quad (1)$$

316

317 For equation (1), TEP number concentrations were converted to TEP volume  
318 concentrations. To this end, for atmospheric and for oceanic samples, particle number  
319 concentrations of TEP were extracted from the size distribution spectra and volume  
320 concentrations were calculated (assuming spherical particles). More detail on the conversion  
321 can be found in the SI (Tab. S2-S5).

322

### 323 3 Results and Discussion

#### 324 3.1 Concentration and size distribution of TEP

325 Within the three-weeks sampling period, TEP varied within one order of magnitude between  
326  $7 \times 10^2$  and  $3 \times 10^4$  #TEP  $m^{-3}$  in the aerosol particles and between  $4 \times 10^6$  and  $9 \times 10^6$  #TEP  $L^{-1}$  in the  
327 cloud water (analysed diameter size range:  $\sim 4.5$  to  $\sim 30$   $\mu m$ ) as shown in **Fig. 2**. The cloud  
328 water concentrations were converted to atmospheric concentrations using the measured LWC  
329 of the cloud water ( $0.39$   $g\ m^{-3}$ ) and resulted in concentrations of  $2 - 4 \times 10^3$  #TEP  $m^{-3}$  (**Tab. S4**).  
330 As a result, a striking similarity (agreement within one order of magnitude) for TEP  
331 concentrations in the aerosol particles (average:  $1 \times 10^4$  #TEP  $m^{-3}$ , Tab. S2) and the cloud water  
332 (average:  $0.3 \times 10^4$  #TEP  $m^{-3}$ , Tab. S4) was found, suggesting that the majority of the TEP  
333 particles are activated to cloud droplets when a cloud forms.

334 **Insert Figure 2**

335

336 In addition, TEP were measured in four aerosol particle samples from the plunging  
337 waterfall tank and the concentrations varied between  $4 \times 10^2$  and  $3 \times 10^3$  #TEP  $m^{-3}$  (**Tab. S3**).  
338 While the TEP concentrations in ambient aerosol particle and cloud water were not  
339 significantly different (ANOVA, oneway,  $p = 0.054$  at a 0.05 level), the tank-generated TEP



340 concentrations were significantly lower than the ambient aerosol TEP concentrations (ANOVA,  
341 oneway,  $p = 0.004$  at a 0.05 level). The TEP number concentrations measured in the different  
342 atmospheric compartments, the ambient aerosol particles, the tank-generated aerosol  
343 particles and the cloud water are summarized in **Fig. 3a** and the individual values are  
344 presented in the **Tab. S2-S4**.

345 *Insert Figure 3*

346

347 Besides for the total number concentrations, TEP number size distribution were  
348 derived from all ambient aerosol particle samples and are shown in **Fig. 4 (a-d)** in both, linear  
349 and logarithmic form. In addition, the TEP number size distribution of one cloud water sample  
350 is presented in **Fig. 4 (e, f)**. All samples exhibited very similar trends in their size distribution,  
351 with higher number concentrations for smaller sizes.

352 *Insert Figure 4*

353

354 From the observed size distributions, it can be assumed that the number  
355 concentrations will continue to increase toward smaller sizes. A comparison of TEP number  
356 concentrations in the ambient aerosol particles or cloud water to literature values is  
357 challenging due to the availability of very few studies and different sample types and size  
358 ranges regarded in different studies. However, the here observed trend in the TEP number  
359 size distributions is consistent with studies from Kuznetsova et al. (2005) showing increased  
360 TEP concentrations in simulated sea spray regarding particle sizes from 50  $\mu\text{m}$  to 10  $\mu\text{m}$  in  
361 diameter. In addition, TEP mass concentrations showed a similar trend with higher  
362 concentrations towards smaller particle sizes (size range 0.1-1  $\mu\text{m}$ , Aller et al. (2017)), that  
363 was, however not as pronounced as for TEP number concentrations observed here.

364 Regarding polymer gels in general, a strong increase with decreasing sizes was  
365 observed for the polymer gels in cloud water in the high Arctic (north of 80°N) in late summer  
366 using a very sensitive microscopic technique with epifluorescence (Orellana et al., 2011).  
367  $2 \times 10^9$  micrometer-sized polymer gels per  $\text{mL}^{-1}$  and  $2 - 6 \times 10^{11}$  nanometer-sized polymer gels  
368 per  $\text{mL}^{-1}$  were observed and the majority of the particles were smaller than 100 nm (Orellana  
369 et al., 2011). The measurements from Orellana et al. (2011) regarded a much smaller particle  
370 diameter range (down to nm scale) compared to the present work and are therefore not  
371 directly comparable. However, from the logarithmic TEP number concentration vs. diameter  
372 relationship (**Fig.4**) we calculated TEP number concentrations for smaller particle ranges (sub-  
373 micrometer size range). TEP number concentrations between  $4.2 \times 10^4$  #TEP  $\text{m}^{-3}$  (low “TEP5”  
374 case, equation from **Fig. 4b**) and  $1.6 \times 10^6$  #TEP  $\text{m}^{-3}$  (high “TEP10” case, equation from **Fig. 4d**)  
375 are calculated for  $\text{PM}_1$  particles. The high but varying concentrations for the two cases  
376 underlines the need for more measurements in the submicron range to derive robust  
377 numbers. Similarly, a concentration of  $3.0 \times 10^8$  #TEP  $\text{L}^{-1}$  for  $\text{PM}_1$  particles in cloud water were



378 calculated and  $2.1 \times 10^{10}$  #TEP  $L^{-1}$  for  $PM_{0.2}$  particles might exist in the submicron-size range  
379 (following the equation from Fig. 4f).

380 These calculations show that the number of gel-like particles in the high Arctic was still  
381 several orders of magnitudes higher compared to TEP particles in the tropical Atlantic, e.g.  
382  $10^{10}$  #TEP  $L^{-1}$  (200 nm particles) in tropical cloud water observed here vs.  $10^{11}$  #polymer gels  
383 per  $mL^{-1}$  ( $= 10^{14}$  #polymer gels per  $L^{-1}$ ) from Orellana et al. (2011). If the TEP particles in the  
384 tropical atmosphere comprise only a small subgroup of the total polymer gel number, or if the  
385 total amount of gel-like particles is generally higher in Polar Regions remains to be  
386 investigated.

### 387 3.2 Relating atmospheric TEP to the ocean

388 From a recent study of TEP number concentrations in different oceanic regions, TEP number  
389 concentrations in surface waters (10 m depth) of the East Tropical North Atlantic (ETNA) were  
390 obtained (Engel et al., 2020). ETNA is the region that geographically includes the Cape Verde  
391 islands. The oceanic TEP number concentrations are shown in Fig. 5 and are discussed in more  
392 detail in Engel et al. (2020). The TEP in the ocean showed a similar size distribution compared  
393 to the TEP in the atmosphere (i.e. aerosol particles and cloud water, Fig. 4) with increasing  
394 TEP number concentrations toward smaller particle sizes (Tab. S5 and more details in Engel et  
395 al. (2020)).

396

#### 397 *Insert Fig. 5*

398

399 A detailed comparison of #TEP in the ocean and in the atmosphere regarding the  
400 identical size bins showed that the #TEP distribution among the different size bins were much  
401 more balanced for seawater than for aerosol particles. In aerosol particles, on average 51% of  
402 the #TEP were located in the smallest analysed size bin ( $4.5\text{--}7\ \mu m$ ) and show a sharp decrease  
403 towards the second size bin (that contained 24% of the TEP) (Fig. 6). For the seawater TEP,  
404 however, around 35% of the #TEP were found in the first size bin and the relative contribution  
405 decreased uniformly towards the larger size bins (Fig. 6). This distribution is also visible in the  
406 correlation curves of Fig 4 (b,d,f) and Figure 5b. The correlation curves for the aerosol particles  
407 (and cloud water) have a steeper slope compared to the curve obtained for seawater TEP. This  
408 could imply that i) the transfer of TEP from the ocean to the atmosphere is most efficient for  
409 small size ranges, ii) larger TEP are converted to smaller TEP in the atmosphere (e.g. break  
410 down), and /or iii) atmospheric in-situ formation mechanism of TEP preferably occur in smaller  
411 particle size ranges. These considerations will be further evaluated in section 3.3.

412

#### 413 *Insert Figure 6*

414

415 Ocean water, atmospheric particles, and cloud water are different marine  
416 compartments and to compare seawater and atmospheric TEP concentrations in terms of



417 enrichment or depletion, the atmospheric enrichment factor  $EF_{atm.}$  (Equation 1) was  
418 calculated. In order to compare the same TEP diameters in all compartments, the size range  
419 between 5  $\mu\text{m}$  (lower limit for atmospheric measurements) and 10  $\mu\text{m}$  (typical upper limit for  
420 ambient aerosol particles) was regarded and converted from number to volume concentration  
421 (more details in Table S2-S4 and Fig. S1). For ocean water, TEP number concentrations of  
422  $3.5 \times 10^3 \text{ \#TEP mL}^{-1}$  ( $= 3.5 \times 10^6 \text{ \#TEP L}^{-1}$ ) and a TEP volume concentration of  $4.6 \times 10^5 \mu\text{m}^3 \text{ TEP mL}^{-1}$   
423 ( $= 3.5 \times 10^8 \mu\text{m}^3 \text{ TEP L}^{-1}$ ) were obtained. The respective values for the TEP volume  
424 concentration of ambient and tank-generated aerosol particles, as well as for the cloud water  
425 are listed in Tables S2-S4 and illustrated in Fig 3b. The factors given here are subject to some  
426 uncertainties and represent lower limits. An error discussion is introduced in the Supporting  
427 Information as an appendix to Table S2. It is clearly visible that the  $EF_{aer. ambient}$  are significantly  
428 higher than the  $EF_{aer. tank}$  (ANOVA, oneway,  $p = 0.0017$  at a 0.05 level) with average values of  
429  $9 \times 10^3$  and 50, respectively. The average  $EF_{cloud}$  was  $1 \times 10^3$ . This means that the enrichment of  
430 TEP derived from the plunging waterfall tank, representing the bubble-bursting transfer, is  
431 about two orders of magnitude lower compared to the enrichment of TEP in the ambient  
432 aerosol particles. In the following, this finding will be discussed in more detail considering  
433 studies available from literature.

434 Atmospheric enrichment of ocean-derived OM, have often been reported (e.g.  
435 Facchini et al., 2008; Keene et al., 2007; O'Dowd et al., 2004; Schmitt-Kopplin et al.,  
436 2012; Triesch et al., 2021a; Triesch et al., 2021b; van Pinxteren et al., 2017). Submicron particles  
437 are usually strongly enriched with organic matter with aerosol enrichment factors  $EF_{aer.}$  of  $10^3$   
438 up to  $10^5$  (Quinn et al., 2015 and references therein). The enrichment in supermicron aerosol  
439 particles is, however, significantly lower. Laboratory studies showed enrichment of OM in the  
440 order of  $10^2$  (Hoffman and Duce, 1976; Keene et al., 2007; Quinn et al., 2015). From the  
441 MarParCloud campaign, enrichment factors of free amino acids were between 10 and 30 in  
442 ambient supermicron particles (Triesch et al. 2021a). Kuznetsova et al. (2005) reported TEP  
443 enrichments in freshly produced sea spray with  $EF_{aer.} = 44 \pm 22$  based on TEP number  
444 concentration. Consequently the here reported  $EF_{aer. tank}$  ( $50 \pm 35$ ) are well in-line with  
445 published enrichment factors for OM in general and TEP specifically. However, the  $EF_{aer. ambient}$   
446 ( $9 \times 10^3$ ) were orders of magnitude higher than reported enrichment factors for supermicron  
447 aerosol particles. Enrichment factors of OM in cloud water are hardly available; we recently  
448 reported an enrichment of  $10^3 - 10^4$  of free amino acids in cloud water from the MarParCloud  
449 campaign (Triesch et al., 2021a) that were higher than the here observed  $EF_{cloud}$ .

450 The concept of the aerosol enrichment factor originally originates from controlled tank  
451 experiments where a direct transfer of compounds from the ocean via sea-spray aerosol  
452 formation occurs. Obviously, this does not automatically correspond to the ambient  
453 environment as mixing processes, aging, and further transformation reactions are not  
454 accounted for. However, the  $EF_{aer. ambient}$  which is much bigger than  $EF_{aer.}$ ,  $EF_{aer. tank}$  and the  
455 comparison of  $EF_{cloud}$  towards former literature data clearly show the presence of significantly



456 more TEP in ambient aerosol and cloud water compared to oceanic seawater which will be  
457 discussed in detail in the following section.

458

459 3.3 Possible sources and atmospheric formation pathways of TEP

460

461 3.3.1 Primary TEP sources

462

463 The high abundance of TEP in the aerosol particles and cloud water might correspond  
464 to an oceanic transfer within the process of bubble bursting. To investigate a linkage to the  
465 bubble bursting transfer, TEP concentrations were correlated to the sea-spray tracers sodium  
466 and magnesium. To account for biases due to a number-based (TEP) and mass-based (sodium,  
467 magnesium) comparison, the particle volume of TEP was calculated from the particle number  
468 concentrations (regarding the size range: 5-10  $\mu\text{m}$ ). To this end, from each particle diameter  
469 within a size range of 5-10  $\mu\text{m}$ , the respective volume was determined, assuming spherical  
470 particles, and summed up (data in **Tab. S2**). This transformation accounts for the fact that big  
471 TEP particles likely possess a large mass but a low number concentration and vice versa.

472 Reasonably good correlations of TEP to sodium and magnesium, ( $R^2 = 0.5$ , **Fig. 7a,b**)  
473 suggested some connection to a bubble bursting transfer. This was further supported by a  
474 moderate correlation of  $R^2 = 0.5$  of TEP to sea-salt calcium ( $\text{Ca}_{\text{ss}}$ , **Fig. 7c**), which was absent for  
475 non-sea-salt calcium and total calcium (**Fig. 7d**).

476

477 *Insert Figure 7*

478

479 Despite this correlation of TEP to sea spray tracers, the high abundance and  
480 enrichment of #TEP in the ambient aerosol particles compared to literature data (Kuznetsova  
481 et al., 2005) and compared to the concentration and enrichment of the #TEP from the plunging  
482 waterfall tank performed here, suggests that additional TEP sources in the ambient  
483 atmosphere exist from which TEPs are added to their primary transfer by bubble bursting from  
484 the oceans. At the Cape Verde islands, besides the ocean, mineral dust is an important aerosol  
485 particle source (Fomba et al., 2014). TEP are generally attributed to be ocean-derived  
486 compounds however, dust has often been reported to transport attached biological particles  
487 (Maki et al., 2019; Marone et al., 2020). During the MarParCloud campaign, dust influences  
488 were low to moderate and the aerosol particle mass was found to be predominantly of marine  
489 origin (Fomba et al., 2014; van Pinxteren et al., 2020). Some dust influences were visible  
490 though, e.g. variations in the particle number concentrations, with elevated concentrations  
491 on (even low) dust influenced air masses (Gong et al., 2020b). TEP number concentrations  
492 showed no clear connection to the ambient dust concentrations (**Fig. 2**). Within periods of  
493 moderate dust, TEP were partly below the detection limits (on 26.09.2017) and partly  
494 exhibited high concentrations (e.g. on 28. and 29.09.2017). A correlation between TEP and  
495 dust was not found ( $R^2 = 0.05$ , **Fig. 7e**) therefore, we do not consider dust to be a transport



496 medium for TEP to the particles or cloud water. However, dust might play a role in abiotic TEP  
497 formation, as discussed in chapter 3.3.2.1.

498

499 3.3.2. In-situ formation

500

501 3.3.2.1 Abiotic formation

502

503 In aquatic environments, abiotic TEP formation has been reported to happen via  
504 several pathways, including spontaneous assembly from TEP precursors (Passow, 2002b). The  
505 aerosol particle and cloud water samples from the MarParCloud campaign investigated here  
506 showed high mass concentrations of amino acids (up to  $6.3 \text{ ng m}^{-3}$  in the submicron aerosol  
507 particles and up to  $490 \text{ ng m}^{-3}$  in the cloud water, published in Triesch et al. (2021a)) as well  
508 as dissolved polysaccharides (up to  $2 \text{ ng m}^{-3}$  in the submicron aerosol particles and up to  $2400$   
509  $\text{ng m}^{-3}$  in the cloud water, results in preparation for publication). In the ocean, the dissolved  
510 polysaccharides are known TEP precursors (Passow, 2002b) and Wurl et al. (2011) determined  
511 abiotic TEP formation rates from dissolved polysaccharide concentration in various oceans.  
512 Therefore, spontaneous TEP formation from the (high) abundant dissolved polysaccharides  
513 likely contributed to the high TEP concentrations observed in the ambient atmosphere in the  
514 present study.

515 Another important parameter likely impacting TEP formation is the presence of  
516 mineral dust. As already discussed above, dust mass concentrations were low to moderate,  
517 however not negligible, during the MarParCloud campaign. In laboratory minicosm studies,  
518 the addition of dust to oceanic water resulted in an acceleration of the kinetics of TEP  
519 formation leading to the formation of fast sinking particles (Louis et al., 2017). This process  
520 likely happens due to particle aggregation, meaning that dissolved OM and dust aggregate to  
521 form TEP (Louis et al., 2017). In addition, dust particles in cloud water might promote  
522 turbulence, which, in aquatic media, has been suggested to enhance abiotic TEP formation  
523 (Passow, 2002b). The dust deposition at the Cape Verdes has been recognized as a potentially  
524 large contributing factor to the TEP enrichment in the SML at the Cape Verdes (Robinson et  
525 al., 2019a). Here, we speculate that even low concentrations of mineral dust can influence the  
526 TEP formation on the aerosol particles and in the cloud water. This is further supported by the  
527 microscopic detection of dust in the cloud water (**Fig. 1**), that likely enhance the possibility  
528 that particles in the cloud water collide and stick. Consequently, while dust did not seem to  
529 serve as a transport medium for TEP (see sec. 3.3.1), dust may contribute to in-situ TEP  
530 formation in cloud water due to abiotic particle aggregation.

531 From atmospheric studies, marine gel particles have been reported to undergo a  
532 volume phase transition in response to environmental stimuli, such as pH and temperature as  
533 well as cleavage of their polymers due to UV radiation (Orellana et al., 2011). UV radiation can  
534 break down microgels in the ocean to a high number of smaller (nano-sized) particles (Orellana  
535 and Verdugo, 2003) – a mechanism that is expected highly relevant in the atmosphere where



536 UV radiation is higher than in seawater. Furthermore, it has been shown that a lowering of  
537 the pH from neutral conditions (7 or 8) to 4.5 causes a sudden transition of gel particles in  
538 which the polymer network collapsed to a dense, non-porous array (Chin et al., 1998). The pH  
539 in the cloud water analysed here was between 6.3 and 6.6. As TEP are reported to exhibit a  
540 gel-like character (Passow, 2002b), volume and number concentrations might be affected by  
541 the different pH, ion density, temperature and pressure in the atmosphere. At cloud water  
542 pH-values such as measured here, marine gels have been found to split into smaller units (Chin  
543 et al., 1998), that are below the minimum detectable particle size of 4.5  $\mu\text{m}$ . This could explain  
544 the lower concentrations in cloud water ( $2 - 4 \times 10^3 \text{ \#TEP m}^{-3}$ ) compared to ambient aerosol  
545 particles ( $7 \times 10^2 - 3 \times 10^4 \text{ \#TEP m}^{-3}$ ). Hence, the different environmental stimuli likely impact  
546 atmospheric TEP formation and might lead to the formation of smaller particles. However,  
547 from our data we cannot report on the quantity of these effects and such investigations  
548 warrant further studies.

#### 549 3.3.2.2 Biotic formation

550

551 Besides abiotic pathways, in aqueous media, TEP can be directly released as  
552 particulates from aquatic organisms involving phytoplankton and bacteria (Passow, 2002a)  
553 Biotic TEP formation has by now been studied for seawater and lakes (Passow, 2002a)  
554 however, bacteria are also present in the atmosphere and likely transferred from the ocean  
555 via sea spray (Rastelli et al., 2017) and can survive in cloud droplets (Deguillaume and al.,  
556 2020). The bacterial abundance in cloud water samples taken at Mt. Verde during the  
557 MarParCloud campaign ranged between 0.4 and  $1.5 \times 10^5 \text{ cells mL}^{-1}$  (van Pinxteren et al., 2020).  
558 This concentration is one to two orders of magnitude higher than the TEP concentrations. The  
559 bacterial tracer muramic acid (Mimura and Romano, 1985) was detected in the aerosol  
560 particles and cloud water sampled here in considerable concentrations ( $\sim 25 \text{ nM}$ , data not  
561 shown), strongly suggesting bacterial activity in cloud water. We cannot derive conclusions on  
562 the origin of the bacteria measured in cloud water reported here, however the transfer of  
563 bacteria from the ocean to the atmosphere has been shown before (Rastelli et al.,  
564 2017; Uetake et al., 2020). TEP are known to be closely connected to bacteria in different ways  
565 (Passow, 2002b; Passow, 2002a), therefore, the presence of bacteria in the atmosphere  
566 exhibits a potential source of cloud water TEP observed here. Furthermore, TEP are strongly  
567 colonized by bacteria (Busch et al., 2017; Zäncker et al., 2019). Hence, TEP can be a transfer  
568 vector for bacteria from the ocean to the atmosphere and/or act as a medium for bacterial  
569 colonisation in marine clouds.

570 The presence of active enzymes on ambient aerosol particles (enriched compared to  
571 seawater) and therefore biogenic in-situ cycling of OM through enzymatic reactions in  
572 atmospheric particles was recently suggested (Malfatti et al., 2019). This is well in-line with  
573 the findings that the aerosol particles and cloud water from the MarParCloud campaign  
574 contained high concentrations of OM (amino acids, lipids), assumingly connected to the  
575 biogenic formation (Triesch et al., 2021a; Triesch et al., 2021b). A combined approach of





576 laboratory experiments and modelling recently underlined the importance of biotic (and  
577 abiotic) formation processes of OM in clouds (Jaber et al., 2021).

578           Considering recent literature and the data reported here, we suggest that in-situ TEP  
579 formation related to biogenic processes and likely connected to bacteria, as reported for  
580 seawater, are important in the marine atmosphere as well.

### 581 3.4 Connecting TEP and Ice nucleating particles (INP)

582           Different kinds of ice-nucleating macromolecules have been found in a certain range  
583 of biological species and consist of a variety of chemical structures including proteins,  
584 polysaccharides (Pummer et al., 2015) and lipids (DeMott et al., 2018). TEP, consisting of  
585 polysaccharidic chains, bridged with divalent cations, may therefore possess good properties  
586 to act as INP, however, such a link has not yet been shown in field experiments.

587           During the MarParCloud campaign INP number concentration ( $N_{INP}$ ) was measured in  
588 different marine compartments and the results are presented in Gong et al. (2020a). By  
589 combining INP concentration in the seawater, aerosol particles and cloud water, it was found  
590 that  $N_{INP}$  in the atmosphere were at least four orders of magnitude higher than what would  
591 be expected if all airborne INP would originate from sea spray. The measurements indicated  
592 that other sources besides the ocean, such as mineral dust or other long-ranged transported  
593 particles, contributed to the local INP concentration. However, some indications for  
594 contributions of biological particles to the INP population were obtained (details in Gong et  
595 al., 2020a). Nevertheless, the sources of INP could not be revealed in detail.

596           In the present study, quantitative INP data (presented in Gong et al. 2020a) and TEP  
597 data measured from the same campaign were compared. To this end, INP concentrations  
598 achieved from PM<sub>10</sub> quartz-fiber filters taken at the CVAO during the same period as the TSP  
599 filters were compared with the TEP measurements. In addition, cloud water INP and TEP data  
600 obtained from the same samples were combined.

601           TEP number concentrations were on average between  $10^3 - 10^4 \text{ m}^{-3}$  in the ambient  
602 aerosol particles, whereas INP number concentrations at  $-15 \text{ }^\circ\text{C}$  were between  $10 - 10^2 \text{ m}^{-3}$   
603 (Gong et al., 2020a). It is interesting to note that the TEP concentrations in the ambient aerosol  
604 particles were about two orders of magnitude higher compared to INP concentrations. Similar  
605 findings were obtained for the cloud water comparisons; TEP concentrations ( $\sim 10^6 \text{ L}^{-1}$ ) were  
606 on average two orders of magnitude higher than INP number concentrations at  $-15 \text{ }^\circ\text{C}$  in cloud  
607 water ( $\sim 10^4 \text{ L}^{-1}$ ) (Gong et al., 2020a).

608           The correlation between INP (active at  $-15^\circ\text{C}$ ) and TEP concentrations was weak with  
609  $R^2 = 0.3$  (Fig. 5f), showing that a direct link between INP and the entire TEP number  
610 concentrations was not very pronounced. It needs to be underlined that TEP concentrations  
611 below a particle size of  $4.5 \mu\text{m}$  are not included here and according to the size distribution,  
612 the TEP concentrations are increasing towards smaller sizes. Most of the here reported TEP  
613 particles were in the supermicron sizes ( $\sim 4.5 - 14 \mu\text{m}$ , Fig. 4). However, the biologically active  
614  $N_{INP}$  at the Cape Verdes were mainly present in the supermicron mode ( $> 1 \mu\text{m}$ ) (Gong et al.,



615 2020a), hence a comparison with the TEP particle concentrations above 5  $\mu\text{m}$  seems justified.  
616 Nevertheless, future studies should concentrate on the exact same size ranges for TEP and  
617 INP.

618 The INP functionalities of biomolecules are not straightforward and whether a  
619 macromolecule acts as INP is depending on many factors, as its size, proper position of  
620 functional groups, and their allocation (Pummer et al., 2015). Typically, not the entire surface  
621 of an INP but rather specific areas (active sites) participates in ice nucleation. This means that  
622 despite TEP likely providing INP properties, only a fraction of TEP, if any, might be able to act  
623 as INP. This hypothesis is supported by the findings that marine gels exhibit hydrophobic and  
624 hydrophilic surface-active segments, strongly suggesting a dichotomous, non-uniform  
625 behaviour of polymer gels (Leck et al., 2013; Orellana et al., 2011; Ovadnevaite et al., 2011). As  
626 mentioned in 3.3.2.1 and 3.3.2.2, TEP are often attached to, or colonized with bacteria.  
627 Bacteria itself, have been shown to provide excellent INP functionalities (Pandey et al., 2016)  
628 and TEP might act as a carrying medium for INP, such as bacteria. Bacteria concentrations  
629 were higher than TEP concentrations and also higher than INP concentrations. However, only  
630 a fraction of all bacteria (0.5 – 25%) is associated with TEP and, vice versa, not all TEP are  
631 colonized by bacteria (Passow, 2002b). There is an indication that especially in oligotrophic  
632 waters, as are the Cape Verde islands, the fraction of bacteria attached to TEP is comparably  
633 low (Schuster and Herndl, 1995). Hence, the concentration range of bacteria-colonized TEP in  
634 relation to INP is worth further consideration. This might help to unravel if a functional  
635 relationship between bacteria-colonized TEP and INP exists and if a certain part of TEP contain  
636 fragments in the biological INP population that, beyond dust, play a role in the Cape Verde  
637 atmosphere.

638

#### 639 4 Conclusion

640

641 This study presented TEP number concentrations  $> 4.5 \mu\text{m}$  in ambient atmospheric samples  
642 from the tropical Atlantic Ocean during the MarParCloud campaign as well as in generated  
643 atmospheric particles using a plunging waterfall tank. The atmospheric TEP showed a similar  
644 size distribution compared to the TEP in the ocean with increasing TEP number concentrations  
645 toward smaller particle sizes, however the #TEP distribution among the different size bins  
646 were much more balanced for seawater than for aerosol particles where half of the #TEP were  
647 located in the smallest analysed size bin (4.5-7  $\mu\text{m}$ ). Based on  $\text{Na}^+$  concentrations in sea water  
648 and the atmosphere, the enrichment of TEP in the tank generated aerosol particles was well  
649 in-line with another study. The TEP enrichments in the ambient atmosphere were, however,  
650 up to two orders of magnitude higher compared to the tank study and such high values are  
651 thus far not reported for supermicron aerosol particles. We speculate that the high  
652 enrichment of TEP in supermicron particles and in cloud water result from a combination of  
653 enrichment during bubble-bursting transfer from the ocean and in-situ atmospheric  
654 formation. We propose that similar (biotic and abiotic) formation mechanism reported for TEP



655 formation in the (sea)water might take place in the atmosphere as well, as the required  
656 conditions (e.g. high concentrations of dissolved TEP precursors such as polysaccharides,  
657 presence of bacteria in the cloud water) were given. An assessment of the importance of the  
658 biotic versus the abiotic TEP formation pathways in the atmosphere, however, needs further  
659 investigations. TEP concentrations in the atmosphere were two orders of magnitude higher  
660 than INP concentrations in the aerosol particles and cloud water, respectively. However, only  
661 a part of the TEP population, assumingly the one colonized by bacteria, might contribute to  
662 INP population, and are worth further studies. Finally, while dust might be a dominant INP  
663 source in the here investigated tropical Atlantic region close to the Saharan desert, in other  
664 remote oceanic locations, marine gel particles, their in-cloud formation and connection to  
665 bacteria in the atmosphere could be highly relevant for a better understanding of marine  
666 cloud properties.

667

668 Data availability

669 The data are currently made available through the World Data Centre PANGAEA and the link  
670 will be included in the next version of the manuscript. INP concentrations are accessible under  
671 the following link: <https://doi.pangaea.de/10.1594/PANGAEA.906946>.

672 Special issue statement

673 Acknowledgement

674 We acknowledge the funding by the Leibniz Association SAW in the project “Marine biological  
675 production, organic aerosol particles and marine clouds: a Process Chain (MarParCloud)”  
676 (SAW-2016-TROPOS-2), the Research and Innovation Staff Exchange EU project MARSU  
677 (69089) and the Deutsche Forschungsgemeinschaft (DFG, German Research Foundation) –  
678 Projektnummer 268020496 – TRR 172, within the Transregional Collaborative Research  
679 Center “Arctic Amplification: Climate Relevant Atmospheric and SurfaCe Processes, and  
680 Feedback Mechanisms (AC)<sup>3</sup>” in sub-projects B04. We thank the CVAO site manager Luis Neves  
681 as well as René Rabe and Susanne Fuchs for technical and laboratory assistance. We further  
682 acknowledge the professional support provided by the Ocean Science Centre Mindelo (OSCM)  
683 and the Instituto do Mar (IMar).

684

685 Author contributions

686 MvP led the MarParCloud campaign and, together with the campaign participants KWF, XG,  
687 EB, NT, BR, FS and HW performed the aerosol particle and cloud water sampling at the Cape  
688 Verde island. EB designed and operated the plunging waterfall tank. BR performed the  
689 microscopic TEP measurements and XG made the INP analysis. AE contributed the seawater  
690 TEP data. MvP performed the data interpretation with help from SZ and BR. MvP wrote the  
691 manuscript with contributions from all authors.



692 Competing interest

693 The authors declare that they have no conflict of interest.

694

695 References

696 Alldredge, A. L., Passow, U., and Logan, B. E.: The abundance and significance of a class of  
697 large, transparent organic particles in the ocean Deep-Sea Research Part I-Oceanographic Research  
698 Papers, 40, 1131-1140, 10.1016/0967-0637(93)90129-q, 1993.

699 Aller, J. Y., Radway, J. C., Kilthau, W. P., Bothe, D. W., Wilson, T. W., Vaillancourt, R. D., Quinn,  
700 P. K., Coffman, D. J., Murray, B. J., and Knopf, D. A.: Size-resolved characterization of the  
701 polysaccharidic and proteinaceous components of sea spray aerosol, *Atmos. Environ.*, 154, 331-347,  
702 10.1016/j.atmosenv.2017.01.053, 2017.

703 Bigg, E. K., and Leck, C.: The composition of fragments of bubbles bursting at the ocean  
704 surface, *Journal of Geophysical Research-Atmospheres*, 113, 10.1029/2007jd009078, 2008.

705 Bittar, T. B., Passow, U., Hamaraty, L., Bidle, K. D., and Harvey, E. L.: An updated method for  
706 the calibration of transparent exopolymer particle measurements, *Limnol. Oceanogr. Meth.*, 16, 621-  
707 628, 10.1002/lom3.10268, 2018.

708 Blanchard, D. C.: Bubble Scavenging and the Water-to-Air Transfer of Organic Material in the  
709 Sea, in: *Applied Chemistry at Protein Interfaces, Advances in Chemistry*, 145, American Chemical  
710 Society, 360-387, 1975.

711 Burrows, S. M., Hoose, C., Poschl, U., and Lawrence, M. G.: Ice nuclei in marine air: biogenic  
712 particles or dust?, *Atmospheric Chemistry and Physics*, 13, 245-267, 10.5194/acp-13-245-2013, 2013.

713 Busch, K., Endres, S., Iversen, M. H., Michels, J., Nothig, E. M., and Engel, A.: Bacterial  
714 Colonization and Vertical Distribution of Marine Gel Particles (TEP and CSP) in the Arctic Fram Strait,  
715 *Frontiers in Marine Science*, 4, 10.3389/fmars.2017.00166, 2017.

716 Carpenter, L. J., Fleming, Z. L., Read, K. A., Lee, J. D., Moller, S. J., Hopkins, J. R., Purvis, R. M.,  
717 Lewis, A. C., Müller, K., Heinold, B., Herrmann, H., Fomba, K. W., van Pinxteren, D., Müller, C., Tegen,  
718 I., Wiedensohler, A., Müller, T., Niedermeier, N., Achterberg, E. P., Patey, M. D., Kozlova, E. A.,  
719 Heimann, M., Heard, D. E., Plane, J. M. C., Mahajan, A., Oetjen, H., Ingham, T., Stone, D., Whalley, L.  
720 K., Evans, M. J., Pilling, M. J., Leigh, R. J., Monks, P. S., Karunaharan, A., Vaughan, S., Arnold, S. R.,  
721 Tschrirter, J., Pohler, D., Friess, U., Holla, R., Mendes, L. M., Lopez, H., Faria, B., Manning, A. J., and  
722 Wallace, D. W. R.: Seasonal characteristics of tropical marine boundary layer air measured at the  
723 Cape Verde Atmospheric Observatory, *Journal of Atmospheric Chemistry*, 67, 87-140,  
724 10.1007/s10874-011-9206-1, 2010.

725 Chin, W. C., Orellana, M. V., and Verdugo, P.: Spontaneous assembly of marine dissolved  
726 organic matter into polymer gels, *Nature*, 391, 568-572, 10.1038/35345, 1998.

727 Creamean, J. M., Cross, J. N., Pickart, R., McRaven, L., Lin, P., Pacini, A., Hanlon, R., Schmale, D.  
728 G., Cenicerros, J., Aydell, T., Colombi, N., Bolger, E., and DeMott, P. J.: Ice Nucleating Particles Carried



- 729 From Below a Phytoplankton Bloom to the Arctic Atmosphere, *Geophysical Research Letters*, 46,  
730 8572-8581, 10.1029/2019gl083039, 2019.
- 731 Decho, A. W., and Gutierrez, T.: Microbial Extracellular Polymeric Substances (EPSs) in Ocean  
732 Systems, *Frontiers in Microbiology*, 8, 10.3389/fmicb.2017.00922, 2017.
- 733 Deguillaume, L., and al., e.: Biological Activity in Clouds: From the Laboratory to the Model, in:  
734 Air Pollution Modeling and its Application XXVI. ITM 2018., edited by: Mensink C., G. W., Hakami A. ,  
735 pringer Proceedings in Complexity. Springer, Cham, 2020.
- 736 DeMott, P. J., Mason, R. H., McCluskey, C. S., Hill, T. C. J., Perkins, R. J., Desyaterik, Y., Bertram,  
737 A. K., Trueblood, J. V., Grassian, V. H., Qiu, Y. Q., Molinero, V., Tobo, Y., Sultana, C. M., Lee, C., and  
738 Prather, K. A.: Ice nucleation by particles containing long-chain fatty acids of relevance to freezing by  
739 sea spray aerosols, *Environmental Science-Processes & Impacts*, 20, 1559-1569,  
740 10.1039/c8em00386f, 2018.
- 741 Demoz, B. B., Collett, J. L., and Daube, B. C.: On the Caltech Active Strand Cloudwater  
742 Collectors, *Atmos Res*, 41, 47-62, Doi 10.1016/0169-8095(95)00044-5, 1996.
- 743 Engel, A., Goldthwait, S., Passow, U., and Alldredge, A.: Temporal decoupling of carbon and  
744 nitrogen dynamics in a mesocosm diatom bloom, *Limnology and Oceanography*, 47, 753-761,  
745 10.4319/lo.2002.47.3.0753, 2002.
- 746 Engel, A., Delille, B., Jacquet, S., Riebesell, U., Rochelle-Newall, E., Terbruggen, A., and  
747 Zondervan, I.: Transparent exopolymer particles and dissolved organic carbon production by  
748 *Emiliania huxleyi* exposed to different CO<sub>2</sub> concentrations: a mesocosm experiment, *Aquatic  
749 Microbial Ecology*, 34, 93-104, 10.3354/ame034093, 2004.
- 750 Engel, A.: Determination of Marine Gel Particles in: Practical guidelines for the analysis of  
751 seawater, edited by: [u.a.], O. W. B. R., CRC Press, 2009.
- 752 Engel, A., Endres, S., Galgani, L., and Schartau, M.: Marvelous Marine Microgels: On the  
753 Distribution and Impact of Gel-Like Particles in the Oceanic Water-Column, *Frontiers in Marine  
754 Science*, 7, 10.3389/fmars.2020.00405, 2020.
- 755 Ervens, B., and Amato, P.: The global impact of bacterial processes on carbon mass,  
756 *Atmospheric Chemistry and Physics*, 20, 1777-1794, 10.5194/acp-20-1777-2020, 2020.
- 757 Facchini, M. C., Rinaldi, M., Decesari, S., Carbone, C., Finessi, E., Mircea, M., Fuzzi, S., Ceburnis,  
758 D., Flanagan, R., Nilsson, E. D., de Leeuw, G., Martino, M., Woeltjen, J., and O'Dowd, C. D.: Primary  
759 submicron marine aerosol dominated by insoluble organic colloids and aggregates, *Geophysical  
760 Research Letters*, 35, 10.1029/2008gl034210, 2008.
- 761 Fomba, K. W., Müller, K., van Pinxteren, D., and Herrmann, H.: Aerosol size-resolved trace  
762 metal composition in remote northern tropical Atlantic marine environment: case study Cape Verde  
763 islands, *Atmospheric Chemistry and Physics*, 13, 4801-4814, 10.5194/acp-13-4801-2013, 2013.
- 764 Fomba, K. W., Mueller, K., van Pinxteren, D., Poulain, L., van Pinxteren, M., and Herrmann, H.:  
765 Long-term chemical characterization of tropical and marine aerosols at the Cape Verde Atmospheric  
766 Observatory (CVAO) from 2007 to 2011, *Atmospheric Chemistry and Physics*, 14, 8883-8904,  
767 10.5194/acp-14-8883-2014, 2014.



- 768 Gao, Q., Leck, C., Rauschenberg, C., and Matrai, P. A.: On the chemical dynamics of  
769 extracellular polysaccharides in the high Arctic surface microlayer, *Ocean Sci.*, 8, 401-418,  
770 10.5194/os-8-401-2012, 2012.
- 771 Gong, X. D., Wex, H., van Pinxteren, M., Triesch, N., Fomba, K. W., Lubitz, J., Stolle, C.,  
772 Robinson, T. B., Muller, T., Herrmann, H., and Stratmann, F.: Characterization of aerosol particles at  
773 Cabo Verde close to sea level and at the cloud level - Part 2: Ice-nucleating particles in air, cloud and  
774 seawater, *Atmospheric Chemistry and Physics*, 20, 1451-1468, 10.5194/acp-20-1451-2020, 2020a.
- 775 Gong, X. D., Wex, H., Voigtlander, J., Fomba, K. W., Weinhold, K., van Pinxteren, M., Henning,  
776 S., Muller, T., Herrmann, H., and Stratmann, F.: Characterization of aerosol particles at Cabo Verde  
777 close to sea level and at the cloud level - Part 1: Particle number size distribution, cloud condensation  
778 nuclei and their origins, *Atmospheric Chemistry and Physics*, 20, 1431-1449, 10.5194/acp-20-1431-  
779 2020, 2020b.
- 780 Hartmann, M., Adachi, K., Eppers, O., Haas, C., Herber, A., Holzinger, R., Hunerbein, A., Jakel,  
781 E., Jentzsch, C., van Pinxteren, M., Wex, H., Willmes, S., and Stratmann, F.: Wintertime Airborne  
782 Measurements of Ice Nucleating Particles in the High Arctic: A Hint to a Marine, Biogenic Source for  
783 Ice Nucleating Particles, *Geophysical Research Letters*, 47, 10.1029/2020gl087770, 2020.
- 784 Hoffman, E. J., and Duce, R. A.: Factors influencing organic-carbon content of marine aerosols -  
785 Laboratory study, *J. Geophys. Res.*, 81, 3667-3670, 1976.
- 786 Jaber, S., Joly, M., Brissy, M., Leremboure, M., Khaled, A., Ervens, B., and Delort, A. M.: Biotic  
787 and abiotic transformation of amino acids in cloud water: experimental studies and atmospheric  
788 implications, *Biogeosciences*, 18, 1067-1080, 10.5194/bg-18-1067-2021, 2021.
- 789 Keene, W. C., Maring, H., Maben, J. R., Kieber, D. J., Pszeny, A. A. P., Dahl, E. E., Izaguirre, M.  
790 A., Davis, A. J., Long, M. S., Zhou, X., Smoydzin, L., and Sander, R.: Chemical and physical  
791 characteristics of nascent aerosols produced by bursting bubbles at a model air-sea interface, *Journal*  
792 *of Geophysical Research-Atmospheres*, 112, 10.1029/2007jd008464, 2007.
- 793 Khaled, A., Zhang, M. H., Amato, P., Delort, A. M., and Ervens, B.: Biodegradation by bacteria in  
794 clouds: an underestimated sink for some organics in the atmospheric multiphase system,  
795 *Atmospheric Chemistry and Physics*, 21, 3123-3141, 10.5194/acp-21-3123-2021, 2021.
- 796 Kuznetsova, M., Lee, C., and Aller, J.: Characterization of the proteinaceous matter in marine  
797 aerosols, *Marine Chemistry*, 96, 359-377, 10.1016/j.marchem.2005.03.007, 2005.
- 798 Leck, C., and Bigg, E. K.: Biogenic particles in the surface microlayer and overlying atmosphere  
799 in the central Arctic Ocean during summer, *Tellus Ser. B-Chem. Phys. Meteorol.*, 57, 305-316,  
800 10.1111/j.1600-0889.2005.00148.x, 2005a.
- 801 Leck, C., and Bigg, E. K.: Source and evolution of the marine aerosol - A new perspective,  
802 *Geophysical Research Letters*, 32, 10.1029/2005gl023651, 2005b.
- 803 Leck, C., Gao, Q., Rad, F. M., and Nilsson, U.: Size-resolved atmospheric particulate  
804 polysaccharides in the high summer Arctic, *Atmospheric Chemistry and Physics*, 13, 12573-12588,  
805 10.5194/acp-13-12573-2013, 2013.



- 806 Louis, J., Pedrotti, M. L., Gazeau, F., and Guieu, C.: Experimental evidence of formation of  
807 Transparent Exopolymer Particles (TEP) and POC export provoked by dust addition under current and  
808 high pCO<sub>2</sub> conditions, *Plos One*, 12, 10.1371/journal.pone.0171980, 2017.
- 809 Maki, T., Lee, K. C., Kawai, K., Onishi, K., Hong, C. S., Kurosaki, Y., Shinoda, M., Kai, K., Iwasaka,  
810 Y., Archer, S. D. J., Lacap-Bugler, D. C., Hasegawa, H., and Pointing, S. B.: Aeolian Dispersal of Bacteria  
811 Associated With Desert Dust and Anthropogenic Particles Over Continental and Oceanic Surfaces,  
812 *Journal of Geophysical Research-Atmospheres*, 124, 5579-5588, 10.1029/2018jd029597, 2019.
- 813 Malfatti, F., Lee, C., Tinta, T., Pendergraft, M. A., Celussi, M., Zhou, Y. Y., Sultana, C. M., Rotter,  
814 A., Axson, J. L., Collins, D. B., Santander, M. V., Morales, A. L. A., Aluwihare, L. I., Riemer, N., Grassian,  
815 V. H., Azam, F., and Prather, K. A.: Detection of Active Microbial Enzymes in Nascent Sea Spray  
816 Aerosol: Implications for Atmospheric Chemistry and Climate, *Environmental Science & Technology*  
817 *Letters*, 6, 171-177, 10.1021/acs.estlett.8b00699, 2019.
- 818 Mari, X., Passow, U., Migon, C., Burd, A. B., and Legendre, L.: Transparent exopolymer  
819 particles: Effects on carbon cycling in the ocean, *Progress in Oceanography*, 151, 13-37,  
820 10.1016/j.pocean.2016.11.002, 2017.
- 821 Marone, A., Kane, C. T., Mbengue, M., Jenkins, G. S., Niang, D. N., Drame, M. S., and Gernand,  
822 J. M.: Characterization of Bacteria on Aerosols From Dust Events in Dakar, Senegal, West Africa,  
823 *Geohealth*, 4, 10.1029/2019gh000216, 2020.
- 824 McCluskey, C. S., Hill, T. C. J., Humphries, R. S., Rauker, A. M., Moreau, S., Stratton, P. G.,  
825 Chambers, S. D., Williams, A. G., McRobert, I., Ward, J., Keywood, M. D., Harnwell, J., Ponsonby, W.,  
826 Loh, Z. M., Krummel, P. B., Protat, A., Kreidenweis, S. M., and DeMott, P. J.: Observations of Ice  
827 Nucleating Particles Over Southern Ocean Waters, *Geophysical Research Letters*, 45, 11989-11997,  
828 10.1029/2018gl079981, 2018a.
- 829 McCluskey, C. S., Ovadnevaite, J., Rinaldi, M., Atkinson, J., Belosi, F., Ceburnis, D., Marullo, S.,  
830 Hill, T. C. J., Lohmann, U., Kanji, Z. A., O'Dowd, C., Kreidenweis, S. M., and DeMott, P. J.: Marine and  
831 Terrestrial Organic Ice-Nucleating Particles in Pristine Marine to Continentally Influenced Northeast  
832 Atlantic Air Masses, *Journal of Geophysical Research-Atmospheres*, 123, 6196-6212,  
833 10.1029/2017jd028033, 2018b.
- 834 Mimura, T., and Romano, J. C.: Muramin acid measurements for bacterial investigations in  
835 marine environments by high-pressure-liquid-chromatography, *Applied and Environmental*  
836 *Microbiology*, 50, 229-237, 10.1128/aem.50.2.229-237.1985, 1985.
- 837 Niedermeier, N., Held, A., Müller, T., Heinold, B., Schepanski, K., Tegen, I., Kandler, K., Ebert,  
838 M., Weinbruch, S., Read, K., Lee, J., Fomba, K. W., Müller, K., Herrmann, H., and Wiedensohler, A.:  
839 Mass deposition fluxes of Saharan mineral dust to the tropical northeast Atlantic Ocean: an  
840 intercomparison of methods, *Atmos. Chem. Phys.*, 14, 2245-2266, 10.5194/acp-14-2245-2014, 2014.
- 841 O'Dowd, C. D., Facchini, M. C., Cavalli, F., Ceburnis, D., Mircea, M., Decesari, S., Fuzzi, S., Yoon,  
842 Y. J., and Putaud, J. P.: Biogenically driven organic contribution to marine aerosol, *Nature*, 431, 676-  
843 680, Doi 10.1038/Nature02959, 2004.
- 844 Orellana, M. V., and Verdugo, P.: Ultraviolet radiation blocks the organic carbon exchange  
845 between the dissolved phase and the gel phase in the ocean, *Limnology and Oceanography*, 48,  
846 1618-1623, 10.4319/lo.2003.48.4.1618, 2003.





- 847 Orellana, M. V., Matrai, P. A., Leck, C., Rauschenberg, C. D., Lee, A. M., and Coz, E.: Marine  
848 microgels as a source of cloud condensation nuclei in the high Arctic, *Proceedings of the National*  
849 *Academy of Sciences of the United States of America*, 108, 13612-13617, 10.1073/pnas.1102457108,  
850 2011.
- 851 Ovadnevaite, J., O'Dowd, C., Dall'Osto, M., Ceburnis, D., Worsnop, D. R., and Berresheim, H.:  
852 Detecting high contributions of primary organic matter to marine aerosol: A case study, *Geophysical*  
853 *Research Letters*, 38, 10.1029/2010gl046083, 2011.
- 854 Pandey, R., Usui, K., Livingstone, R. A., Fischer, S. A., Pfaendner, J., Backus, E. H. G., Nagata, Y.,  
855 Frohlich-Nowoisky, J., Schmuser, L., Mauri, S., Scheel, J. F., Knopf, D. A., Pöschl, U., Bonn, M., and  
856 Weidner, T.: Ice-nucleating bacteria control the order and dynamics of interfacial water, *Science*  
857 *Advances*, 2, 10.1126/sciadv.1501630, 2016.
- 858 Passow, U., and Alldredge, A.: A dye-binding assay for the spectrophotometric measurement of  
859 transparent exopolymer particles (TEP), *Limnology and Oceanography*, 40, 10, 1995.
- 860 Passow, U.: Formation of transparent exopolymer particles, TEP, from dissolved precursor  
861 material, *Marine Ecology Progress Series*, 192, 1-11, 10.3354/meps192001, 2000.
- 862 Passow, U.: Production of transparent exopolymer particles (TEP) by phyto- and  
863 bacterioplankton, *Marine Ecology-progress Series - MAR ECOL-PROGR SER*, 236, 1-12,  
864 10.3354/meps236001, 2002a.
- 865 Passow, U.: Transparent exopolymer particles (TEP) in aquatic environments, *Progress in*  
866 *Oceanography*, 55, 287-333, 10.1016/s0079-6611(02)00138-6, 2002b.
- 867 Pummer, B. G., Budke, C., Augustin-Bauditz, S., Niedermeier, D., Felgitsch, L., Kampf, C. J.,  
868 Huber, R. G., Liedl, K. R., Loerting, T., Moschen, T., Schauperl, M., Tollinger, M., Morris, C. E., Wex, H.,  
869 Grothe, H., Pöschl, U., Koop, T., and Frohlich-Nowoisky, J.: Ice nucleation by water-soluble  
870 macromolecules, *Atmospheric Chemistry and Physics*, 15, 4077-4091, 10.5194/acp-15-4077-2015,  
871 2015.
- 872 Quinn, P. K., Collins, D. B., Grassian, V. H., Prather, K. A., and Bates, T. S.: Chemistry and  
873 Related Properties of Freshly Emitted Sea Spray Aerosol, *Chemical Reviews*, 115, 4383-4399,  
874 10.1021/cr500713g, 2015.
- 875 Rastelli, E., Corinaldesi, C., Dell'Anno, A., Lo Martire, M., Greco, S., Facchini, M. C., Rinaldi, M.,  
876 O'Dowd, C., Ceburnis, D., and Danovaro, R.: Transfer of labile organic matter and microbes from the  
877 ocean surface to the marine aerosol: an experimental approach, *Scientific Reports*, 7,  
878 10.1038/s41598-017-10563-z, 2017.
- 879 Robinson, T. B., Stolle, C., and Wurl, O.: Depth is relative: the importance of depth for  
880 transparent exopolymer particles in the near-surface environment, *Ocean Science*, 15, 1653-1666,  
881 10.5194/os-15-1653-2019, 2019a.
- 882 Robinson, T. B., Wurl, O., Bahlmann, E., Juergens, K., and Stolle, C.: Rising bubbles enhance the  
883 gelatinous nature of the air-sea interface, *Limnology and Oceanography*, 64, 2358-2372,  
884 10.1002/lno.11188, 2019b.
- 885 Sander, R., Keene, W. C., Pszenny, A. A. P., Arimoto, R., Ayers, G. P., Baboukas, E., Cainey, J. M.,  
886 Crutzen, P. J., Duce, R. A., Honninger, G., Huebert, B. J., Maenhaut, W., Mihalopoulos, N., Turekian, V.



- 887 C., and Van Dingenen, R.: Inorganic bromine in the marine boundary layer: a critical review,  
888 *Atmospheric Chemistry and Physics*, 3, 1301-1336, 2003.
- 889 Schmitt-Kopplin, P., Liger-Belair, G., Koch, B. P., Flerus, R., Kattner, G., Harir, M., Kanawati, B.,  
890 Lucio, M., Tziotis, D., Hertkorn, N., and Gebeffuegi, I.: Dissolved organic matter in sea spray: a transfer  
891 study from marine surface water to aerosols, *Biogeosciences*, 9, 1571-1582, 10.5194/bg-9-1571-  
892 2012, 2012.
- 893 Schuster, S., and Herndl, G. J.: Formation and significance of transparent exopolymeric  
894 particles in the northern adriatic sea *Marine Ecology Progress Series*, 124, 227-236,  
895 10.3354/meps124227, 1995.
- 896 Sellegrì, K., Nicosia, A., Freney, E., Uitz, J., Thyssen, M., Grégori, G., Engel, A., Zäncker, B.,  
897 Haëntjens, N., Mas, S., Picard, D., Saint-Macary, A., Peltola, M., Rose, C., Trueblood, J., Lefevre, D.,  
898 D'Anna, B., Desboeufs, K., Meskhidze, N., Guieu, C., and Law, C. S.: Surface ocean microbiota  
899 determine cloud precursors, *Scientific Reports*, 11, 281, 10.1038/s41598-020-78097-5, 2021.
- 900 Triesch, N., van Pinxteren, M., Engel, A., and Herrmann, H.: Concerted measurements of free  
901 amino acids at the Cape Verde Islands: High enrichments in submicron sea spray aerosol particles  
902 and cloud droplets, *Atmos. Chem. Phys.*, 21, 163–181, 2021a.
- 903 Triesch, N., van Pinxteren, M., Frka, S., Stolle, C., Spranger, T., Hoffmann, E. H., Gong, X., Wex,  
904 H., Schulz-Bull, D., Gašparović, B., and Herrmann, H.: Concerted measurements of lipids in seawater  
905 and on submicrometer aerosol particles at the Cabo Verde islands: biogenic sources, selective  
906 transfer and high enrichments, *Atmos. Chem. Phys.*, 21, 4267-4283, 10.5194/acp-21-4267-2021,  
907 2021b.
- 908 Turekian, K. K.: *Oceans (Foundations of Earth Science)*, Prentice Hall; 1st Edition, 1968.
- 909 Uetake, J., Hill, T. C. J., Moore, K. A., DeMott, P. J., Protat, A., and Kreidenweis, S. M.: Airborne  
910 bacteria confirm the pristine nature of the Southern Ocean boundary layer, *Proceedings of the*  
911 *National Academy of Sciences of the United States of America*, 117, 13275-13282,  
912 10.1073/pnas.2000134117, 2020.
- 913 van Pinxteren, M., Barthel, S., Fomba, K., Müller, K., von Tümpling, W., and Herrmann, H.: The  
914 influence of environmental drivers on the enrichment of organic carbon in the sea surface microlayer  
915 and in submicron aerosol particles – measurements from the Atlantic Ocean, *Elem Sci Anth*, 5,  
916 <https://doi.org/10.1525/elementa.225>, 2017.
- 917 van Pinxteren, M., Fomba, K. W., Triesch, N., Stolle, C., Wurl, O., Bahlmann, E., Gong, X. D.,  
918 Voigtlander, J., Wex, H., Robinson, T. B., Barthel, S., Zeppenfeld, S., Hoffmann, E. H., Roveretto, M., Li,  
919 C. L., Gosselin, B., Daele, V., Senf, F., van Pinxteren, D., Manzi, M., Zabalegui, N., Frka, S., Gasparovic,  
920 B., Pereira, R., Li, T., Wen, L., Li, J. R., Zhu, C., Chen, H., Chen, J. M., Fiedler, B., Von Tümpling, W.,  
921 Read, K. A., Punjabi, S., Lewis, A. C., Hopkins, J. R., Carpenter, L. J., Peeken, I., Rixen, T., Schulz-Bull,  
922 D., Monge, M. E., Mellouki, A., George, C., Stratmann, F., and Herrmann, H.: Marine organic matter in  
923 the remote environment of the Cape Verde islands - an introduction and overview to the  
924 MarParCloud campaign, *Atmospheric Chemistry and Physics*, 20, 6921-6951, 10.5194/acp-20-6921-  
925 2020, 2020.
- 926 Verdugo, P., Alldredge, A. L., Azam, F., Kirchman, D. L., Passow, U., and Santschi, P. H.: The  
927 oceanic gel phase: a bridge in the DOM–POM continuum, *Marine Chemistry*, 92, 67-85, 2004.



928 Villacorte, L. O., Ekowati, Y., Calix-Ponce, H. N., Schippers, J. C., Amy, G. L., and Kennedy, M. D.:  
929 Improved method for measuring transparent exopolymer particles (TEP) and their precursors in fresh  
930 and saline water, *Water Research*, 70, 300-312, 10.1016/j.watres.2014.12.012, 2015.

931 Wiedensohler, A., Birmili, W., Nowak, A., Sonntag, A., Weinhold, K., Merkel, M., Wehner, B.,  
932 Tuch, T., Pfeifer, S., Fiebig, M., Fjaraa, A. M., Asmi, E., Sellegri, K., Depuy, R., Venzac, H., Villani, P., Laj,  
933 P., Aalto, P., Ogren, J. A., Swietlicki, E., Williams, P., Roldin, P., Quincey, P., Hüglin, C., Fierz-  
934 Schmidhauser, R., Gysel, M., Weingartner, E., Riccobono, F., Santos, S., Gruning, C., Faloon, K.,  
935 Beddows, D., Harrison, R. M., Monahan, C., Jennings, S. G., O'Dowd, C. D., Marinoni, A., Horn, H. G.,  
936 Keck, L., Jiang, J., Scheckman, J., McMurry, P. H., Deng, Z., Zhao, C. S., Moerman, M., Henzing, B., de  
937 Leeuw, G., Loschau, G., and Bastian, S.: Mobility particle size spectrometers: harmonization of  
938 technical standards and data structure to facilitate high quality long-term observations of  
939 atmospheric particle number size distributions, *Atmospheric Measurement Techniques*, 5, 657-685,  
940 10.5194/amt-5-657-2012, 2012.

941 Wilson, T. W., Ladino, L. A., Alpert, P. A., Breckels, M. N., Brooks, I. M., Browse, J., Burrows, S.  
942 M., Carslaw, K. S., Huffman, J. A., Judd, C., Kilhau, W. P., Mason, R. H., McFiggans, G., Miller, L. A.,  
943 Najera, J. J., Polishchuk, E., Rae, S., Schiller, C. L., Si, M., Temprado, J. V., Whale, T. F., Wong, J. P. S.,  
944 Wurl, O., Yakobi-Hancock, J. D., Abbatt, J. P. D., Aller, J. Y., Bertram, A. K., Knopf, D. A., and Murray, B.  
945 J.: A marine biogenic source of atmospheric ice-nucleating particles, *Nature*, 525, 234-+,  
946 10.1038/nature14986, 2015.

947 Wurl, O., and Holmes, M.: The gelatinous nature of the sea-surface microlayer, *Marine*  
948 *Chemistry*, 110, 89-97, 10.1016/j.marchem.2008.02.009, 2008.

949 Wurl, O., Miller, L., and Vagle, S.: Production and fate of transparent exopolymer particles in  
950 the ocean, *J. Geophys. Res.-Oceans*, 116, 10.1029/2011jc007342, 2011.

951 Zäncker, B., Engel, A., and Cunliffe, M.: Bacterial communities associated with individual  
952 transparent exopolymer particles (TEP), *Journal of Plankton Research*, 41, 561-565,  
953 10.1093/plankt/fbz022, 2019.

954 Zeppenfeld, S., van Pinxteren, M., Hartmann, M., Bracher, A., Stratmann, F., and Herrmann, H.:  
955 Glucose as a Potential Chemical Marker for Ice Nucleating Activity in Arctic Seawater and Melt Pond  
956 Samples, *Environmental Science & Technology*, 53, 8747-8756, 10.1021/acs.est.9b01469, 2019.

957 Zeppenfeld, S., van Pinxteren, M., van Pinxteren, D., Wex, H., Berdalet, E., Vaqué, D., Dall'Osto,  
958 M., and Herrmann, H.: Aerosol Marine Primary Carbohydrates and Atmospheric Transformation in  
959 the Western Antarctic Peninsula, *ACS Earth Space Chem.*, 10.1021/acsearthspacechem.0c00351,  
960 2021.

961 Zhang, M. H., Khaled, A., Amato, P., Delort, A. M., and Ervens, B.: Sensitivities to biological  
962 aerosol particle properties and ageing processes: potential implications for aerosol-cloud interactions  
963 and optical properties, *Atmospheric Chemistry and Physics*, 21, 3699-3724, 10.5194/acp-21-3699-  
964 2021, 2021.

965

966

967



968 **Caption of Figures:**

969 **Figure 1:** Microscopic analysis of TEP from the cloud water sample “WW5” (sampling interval:  
970 28.09. 19:30 – 29.09. 7:30 local time). Blue particles are TEP, stained with Alcian Blue solution;  
971 brownish particles in the right picture are assumingly dust particles. The scale refers to 50  $\mu\text{m}$ .  
972

973 **Figure 2:** TEP number concentrations in the aerosol particles (red bars) and in the three cloud  
974 water samples (blue-red squares). TEP concentrations were below the limit of detection (LOD)  
975 on 26th and 27th of September 2017. The backgrounds represent the dust classification  
976 according to the ambient dust concentrations (blue: dust < 5  $\mu\text{g m}^{-3}$  marine conditions; yellow:  
977 dust < 20  $\mu\text{g m}^{-3}$  (low dust); brown: dust < 60  $\mu\text{g m}^{-3}$  (moderate dust). From underlined dates  
978 (22.09 -> “TEP5” and 28.09.2017 -> “TEP10”) TEP number size distributions were measured.  
979

980 **Figure 3:** Box and whisker plot of the TEP number concentrations (a) and the enrichment  
981 factors (b) in the ambient (n=18) and tank-generated (n=4) aerosol particles and in the cloud  
982 water samples (n=3), Each box encloses 50% of the data with the mean value represented as  
983 an open square and the median value represented as a line. The bottom of the box marks the  
984 25% limit of the data, while the top marks the 75% limit. The lines extending from the top and  
985 bottom of each box are the 5% and 95% percentiles within the data set, while the asterisks  
986 indicate the data points lying outside of this range (“outliers”).

987 **Figure 4:** TEP number size distribution in the aerosol particles and cloud water in linear and  
988 logarithmic form; panels (a) and (b) show aerosol particle sample “TEP 5” (sampling start:  
989 22.09.2017), panels (c) and (d) show aerosol sample “TEP 10” (sampling start: 28.09.2017),  
990 panels (e) and (f) show cloud water sample “WW5” (sampling interval: 28.09. 19:30 – 29.09.  
991 7:30 local time). The lower limit of the resolution of the microscope was 16  $\mu\text{m}^2$  resulting in a  
992 particle diameter of 4.5  $\mu\text{m}$  (assuming spherical particle). Each bar in a), c), and e) represents  
993 the summed up particle number concentrations (within 1.5  $\mu\text{m}$ ), e.g. the first column  
994 represents the summed up concentrations between 4.5 and 6  $\mu\text{m}$ .  
995

996 **Figure 5:** TEP number size distributions in the ocean surface water (sampling depth: 10 m)  
997 from the East Tropical North Atlantic (ETNA), averaged over three stations from Engel et al  
998 (2020). The data in this Figure show the size distribution between  $\sim 5$  and  $\sim 30$   $\mu\text{m}$ , matching  
999 the investigated aerosol size range (**Fig. 4**). The whole size spectrum is shown in **Tab. S5**.  
1000

1001 **Figure 6:** Relative contribution of the TEP number concentrations in the aerosol particles  
1002 (left) and in the ocean surface water (right) regarding the identical size bins.

1003



1004 **Figure 7:** Correlations of TEP volume concentrations (size range: 5-10  $\mu\text{m}$ ) to chemical  
1005 parameters (inorganic constituents PM<sub>10</sub>) and dust (PM<sub>10</sub>), as well as correlation of TEP  
1006 number concentration and INP number concentrations. Inorganic constituents were  
1007 measured with ion chromatography and dust concentrations were derived from PM<sub>10</sub>  
1008 concentrations as reported elsewhere (Fomba et al., 2013;van Pinxteren et al., 2020).  
1009 Measurements of INP number concentrations and error bars are explained in (Gong et al.,  
1010 2020a)

1011  
1012  
1013  
1014  
1015  
1016  
1017  
1018  
1019  
1020  
1021  
1022  
1023  
1024  
1025  
1026  
1027  
1028  
1029  
1030  
1031  
1032  
1033  
1034  
1035  
1036  
1037  
1038  
1039  
1040  
1041  
1042  
1043  
1044  
1045  
1046  
1047  
1048  
1049



1050 Table 1. Overview of sampling locations, types and measurements

Sampling site	Campaign	Sample type	Coordinates	No. of samples	Measurements (Particle sizes)
CVAO	MarParCloud 2017	Ambient aerosol particles Inlet height: 42 m a.s.l	16° 51.49' N, 24° 52.02' W	20 20	#TEP (TSP) Inorganic ions (PM <sub>10</sub> )
Mt- Verde	MarParCloud 2017	Ambient cloud water Inlet height: 746 m a.s.l	16°52.11'N, 24°56.02'W	3	#TEP Inorganic ions
Plunging waterfall tank (operated at CVAO)	MarParCloud 2017	Tank-generated aerosol particles	16° 51.49' N, 24° 52.02' W	4	#TEP (TSP) Inorganic ions (TSP)
ETNA (Mauretanian upwelling)	M107 RV Meteor 2012	Ocean surface water	18.00/18.19'N -16.50/72.02'E	6	#TEP

1051

1052

1053

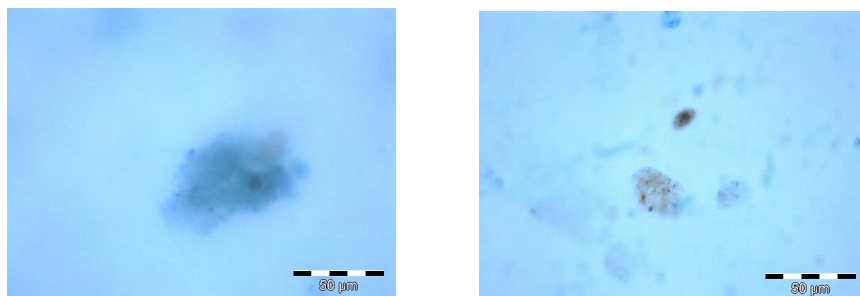
1054

1055



1056

1057



1058

1059

1060

1061

1062

1063

1064

1065

1066

Figure 1



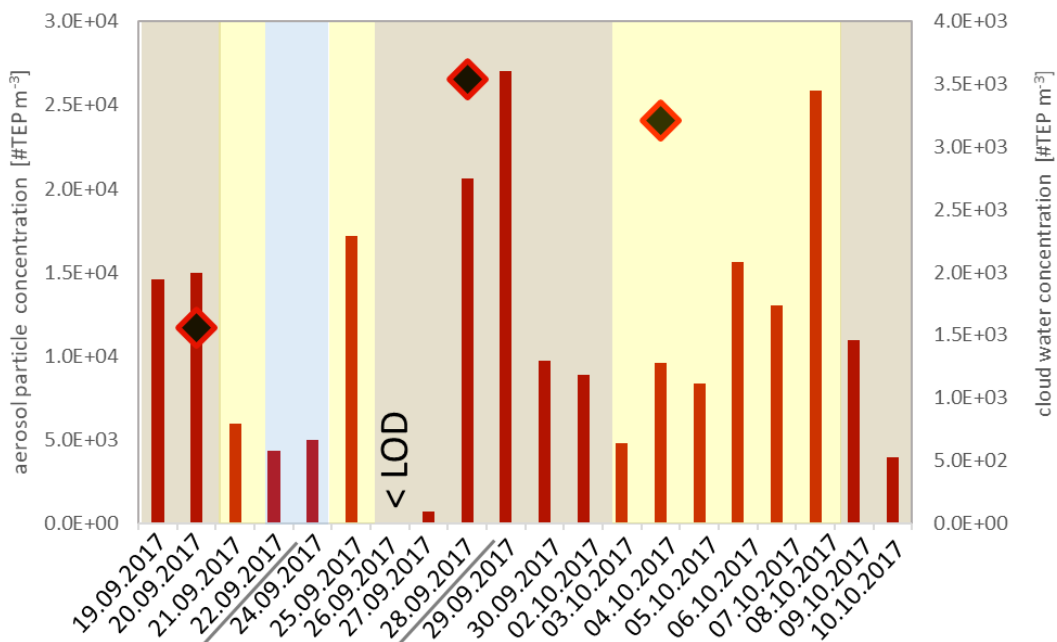


Figure 2

1067  
1068  
1069  
1070  
1071  
1072  
1073  
1074  
1075

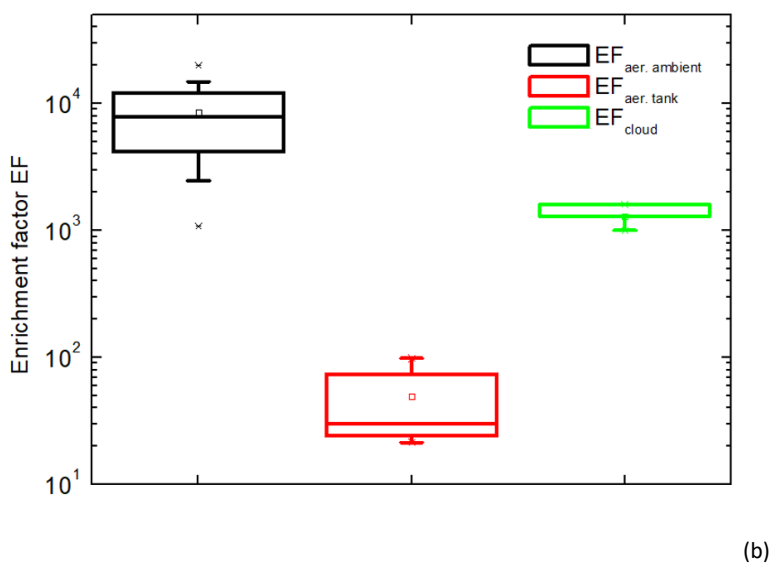
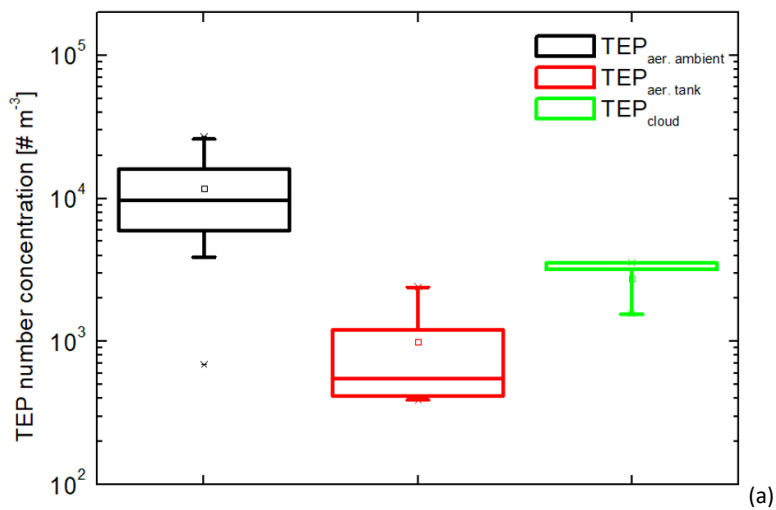


Figure 3

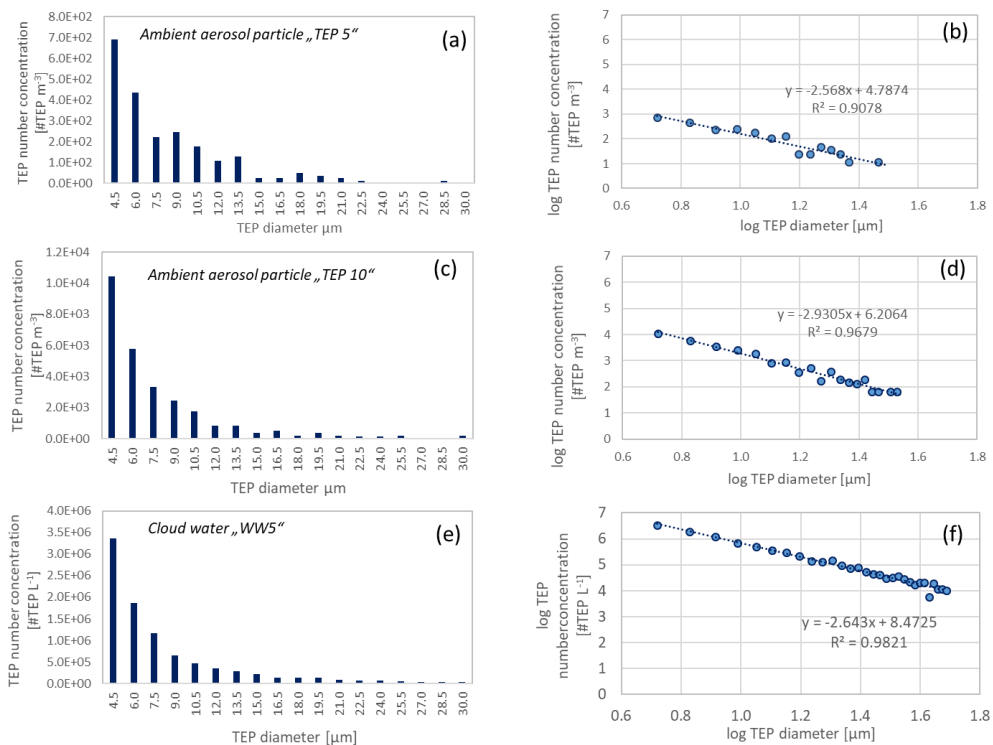
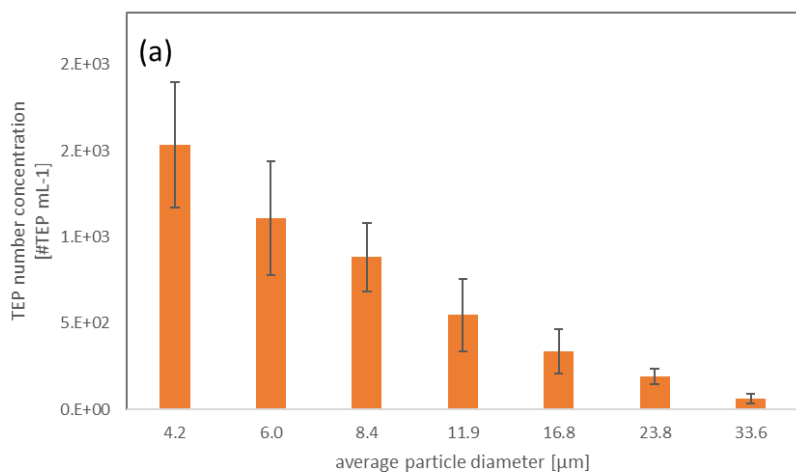


Figure 4

1090  
 1091  
 1092  
 1093  
 1094  
 1095  
 1096



1097

1098

1099

1100

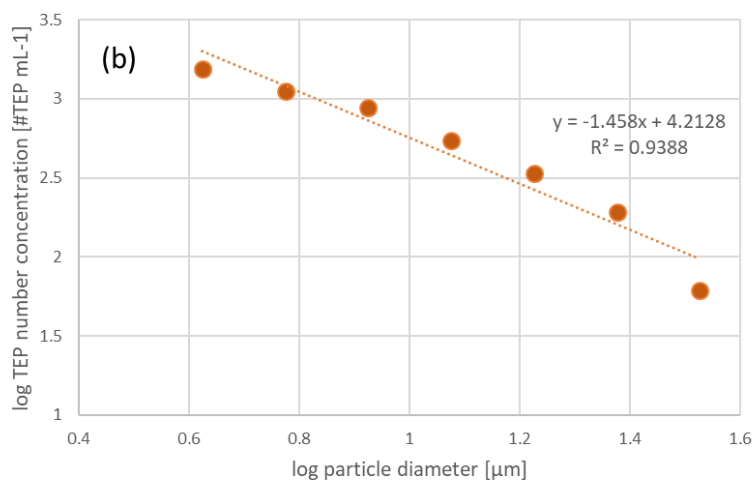
1101

1102

1103

1104

1105



1106

1107

1108

1109

1110

1111

1112

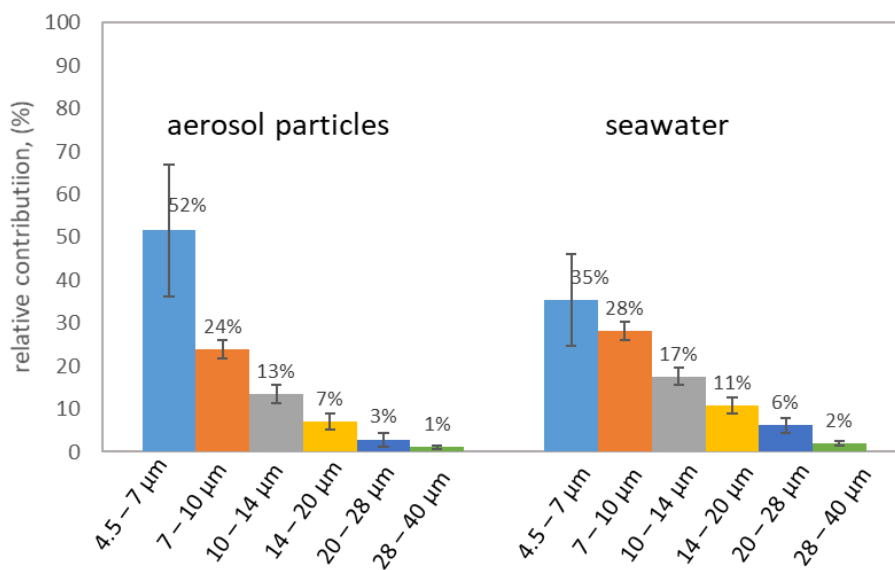
1113

1114

Figure 5



1115



1116

1117

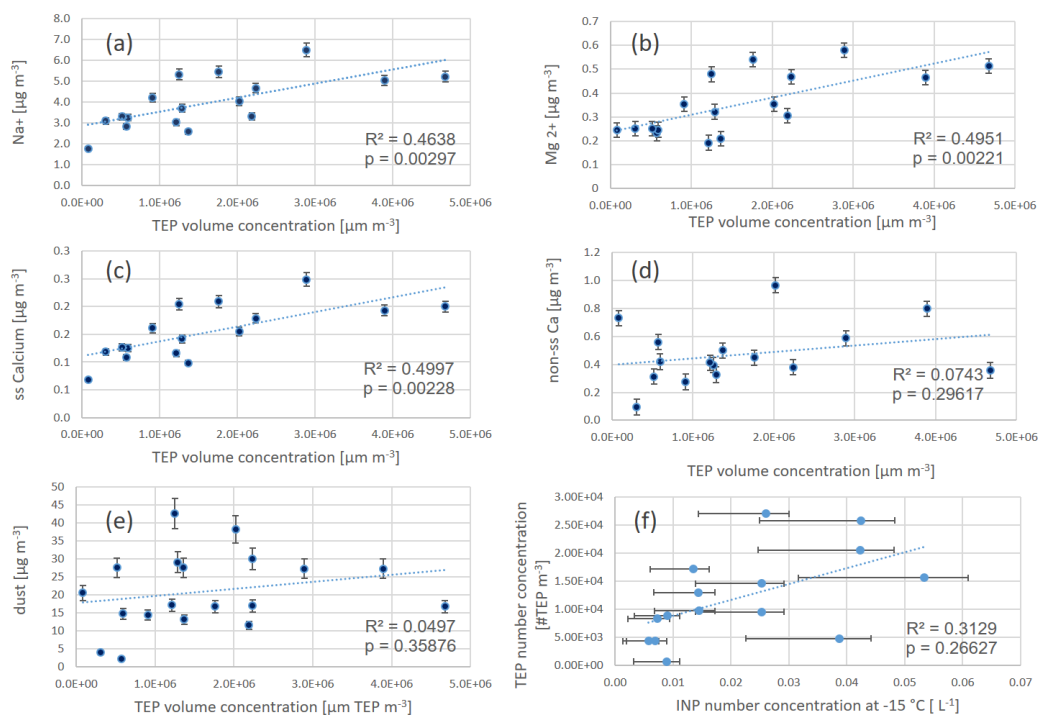
1118

1119

1120

1121

Figure 6



1122

1123

1124

1125

Figure 7